

Thermodynamic study of the CO 2 -H 2 O -NaCl system: Measurements of CO 2 solubility and modeling of phase equilibria using Soreide and Whitson, electrolyte CPA and SIT models

Salaheddine Chabab, Pascal Théveneau, Jérôme Corvisier, Christophe Coquelet, Patrice Paricaud, Celine Houriez, Elise El Ahmar

▶ **To cite this version:**

Salaheddine Chabab, Pascal Théveneau, Jérôme Corvisier, Christophe Coquelet, Patrice Paricaud, et al.. Thermodynamic study of the CO 2 -H 2 O -NaCl system: Measurements of CO 2 solubility and modeling of phase equilibria using Soreide and Whitson, electrolyte CPA and SIT models. International Journal of Greenhouse Gas Control, 2019, 91, pp.102825. 10.1016/j.ijggc.2019.102825 . hal-02310963

HAL Id: hal-02310963
https://hal.science/hal-02310963

Submitted on 10 Oct 2019

HAL is a multi-disciplinary open access archive for the deposit and dissemination of scientific research documents, whether they are published or not. The documents may come from teaching and research institutions in France or abroad, or from public or private research centers.

L'archive ouverte pluridisciplinaire **HAL**, est destinée au dépôt et à la diffusion de documents scientifiques de niveau recherche, publiés ou non, émanant des établissements d'enseignement et de recherche français ou étrangers, des laboratoires publics ou privés.

Thermodynamic study of the CO_2 – H_2O – NaCl system: Measurements of CO_2 solubility and modeling of phase equilibria using Soreide and Whitson, electrolyte CPA and SIT models

Salaheddine Chabab[a], Pascal Theveneau[a], Jérôme Corvisier[b], Christophe Coquelet[a,*], Patrice Paricaud[c], Céline Houriez[a] and Elise El Ahmar[a]

[a]*Mines ParisTech, PSL, CTP - Centre of Thermodynamics of Processes, 35 rue Saint Honoré, 77305 Fontainebleau Cedex, France*

[b]*Mines ParisTech, PSL University, Centre de Géosciences, 35 rue Saint Honoré, 77305 Fontainebleau Cedex, France*

[c]*L'Unité Chimie & Procédés (UCP), ENSTA ParisTech, 828 Boulevard des Maréchaux, 91762 Palaiseau cedex, France*

*Corresponding author. Tel: +33164694962, E-mail address: christophe.coquelet@mines-paristech.fr (C. Coquelet)

Journal: International Journal of Greenhouse Gas Control

Abstract

The thermodynamic study of the CO_2-H_2O-NaCl system is of great importance whether in an environmental context as part of Carbon Capture and Storage (CCS) or in an economic context such as enhanced oil recovery by CO_2 injection, or massive and reversible underground storage for industrial use (methanation, fermentation, water treatment, carbonation of drinks, etc.). In this work, using a new set-up based on the "static-analytic" method, measurements of CO_2 solubility in aqueous sodium chloride solution were performed at molalities between 1 and 3 m, at temperatures between 50 and 100 °C and pressures up to 230 bar. For the modeling part, an electrolyte version of the PR-CPA (Peng-Robinson Cubic Plus Association) equation of state was developed under the name "e-PR-CPA", as well as modified Soreide and Whitson (m-SW) model was used and improved. These two models using the phi-phi approach are compared with two geochemical models (Corvisier 2013 and Duan el al. 2006) using the gamma-phi approach, and against the literature and measured data. The measured data are in good agreement with the literature data and model predictions. Under geological storage conditions, the e-PR-CPA and Duan models estimate solubility slightly better (Average Absolute Deviation less than 6.6%) than the m-SW model and the geochemical model (AAD less than 7.6%).

Keywords: CO_2/brine solubility, CCS, Electrolyte CPA EoS, Measurement, Modeling

1. Introduction

Carbon dioxide emissions, which is the main greenhouse gas (in terms of quantity) produced by human activity, are constantly increasing, mainly due to the exploitation and use of fossil fuels. One of the possible solutions, that is of great interest to industrial actors in the gas sector, is to capture, transport and store carbon dioxide in deep geological formations (salt caverns, saline aquifers, oil and gas fields, etc.). The latter solution can be combined with enhanced oil recovery by CO_2 injection. In an economic context, the reversible storage of carbon dioxide (especially in salt caverns) is also a very good solution to meet the high demand for this gas in many applications (methanation, fermentation, water treatment, carbonation of drinks, etc.).

As part of the ANR FLUIDSTORY[1] project, the feeding of an Electrolysis-Methanation-Oxycombustion (EMO) unit requires massive quantities of CO_2. Therefore, the storage of CO_2 in salt caverns is necessary. Compared to above-ground storage facilities (gas tanks), geological storage facilities are less costly [1] and are protected by a cover rock several hundred meters thick that can withstand high storage pressures [2], which increases the amount of gas stored while maintaining higher safety standards. The design and optimization of the storage facility, as well as the monitoring of the temperature, pressure and quantity of gas in the geological reservoir, require very accurate models under the thermodynamic conditions of the storage.

The presence of brine in salt caverns and deep aquifers completely changes the thermodynamic behavior of the stored gas (salting-out effect) due to the existence of electrolytes (NaCl, KCl, $MgCl_2$, etc.) [3] dissolved in the residual water of the cavern or deep aquifer, so studying these systems becomes very complicated. Na+ and Cl- are the main species found in the salts of most geological formations. The sodium chloride solution is therefore considered to be a representative model of brine [4]. Therefore, the thermodynamic study of the CO_2-H_2O-NaCl ternary system is of great industrial interest.

In the literature, the CO_2-H_2O system is widely studied (experimental measurements and modeling) over a wide temperature and pressure range up to the critical points of the mixture (Todheide and Franck [5] and Takenouchi and Kennedy [6]). At high pressure, the phase equilibria of the CO_2-H_2O-NaCl system is less studied. As a result, recently many studies [7-12]

[1] FluidSTORY project: Massive and reversible underground storage of fluid energy carriers (O_2, CO_2, CH_4).

have been conducted to address the lack of data on this system. In the same way, an experimental apparatus has been developed in this work for the measurement of the solubility of CO_2 in an aqueous solution of sodium chloride, as well as a modeling study for this system was carried out.

This paper is organized as follows: In Section 2 the experimental set-up is described and the measured data are reported. In Section 3, three models are presented, based on two different approaches. The first approach is a symmetric approach (phi-phi) using the same equation of state (EoS) for the two existing phases (liquid-liquid equilibrium and/or vapor-liquid equilibrium); the first equation of state used and improved is the Soreide and Whitson EoS [3]; the second equation of state is an electrolyte version of the PR-CPA EoS which has been developed in this work under the name e-PR-CPA. The second approach tested is an asymmetric approach (gamma-phi) using a geochemical model implemented in the CHESS/HYTEC software (Corvisier, 2013 [13]; Corvisier et al., 2013 [14]). Finally, in Section 4, the results of the three models are presented and compared against literature, measured data, and the well-known DUAN model (Duan et al. [15]).

2. Experimental

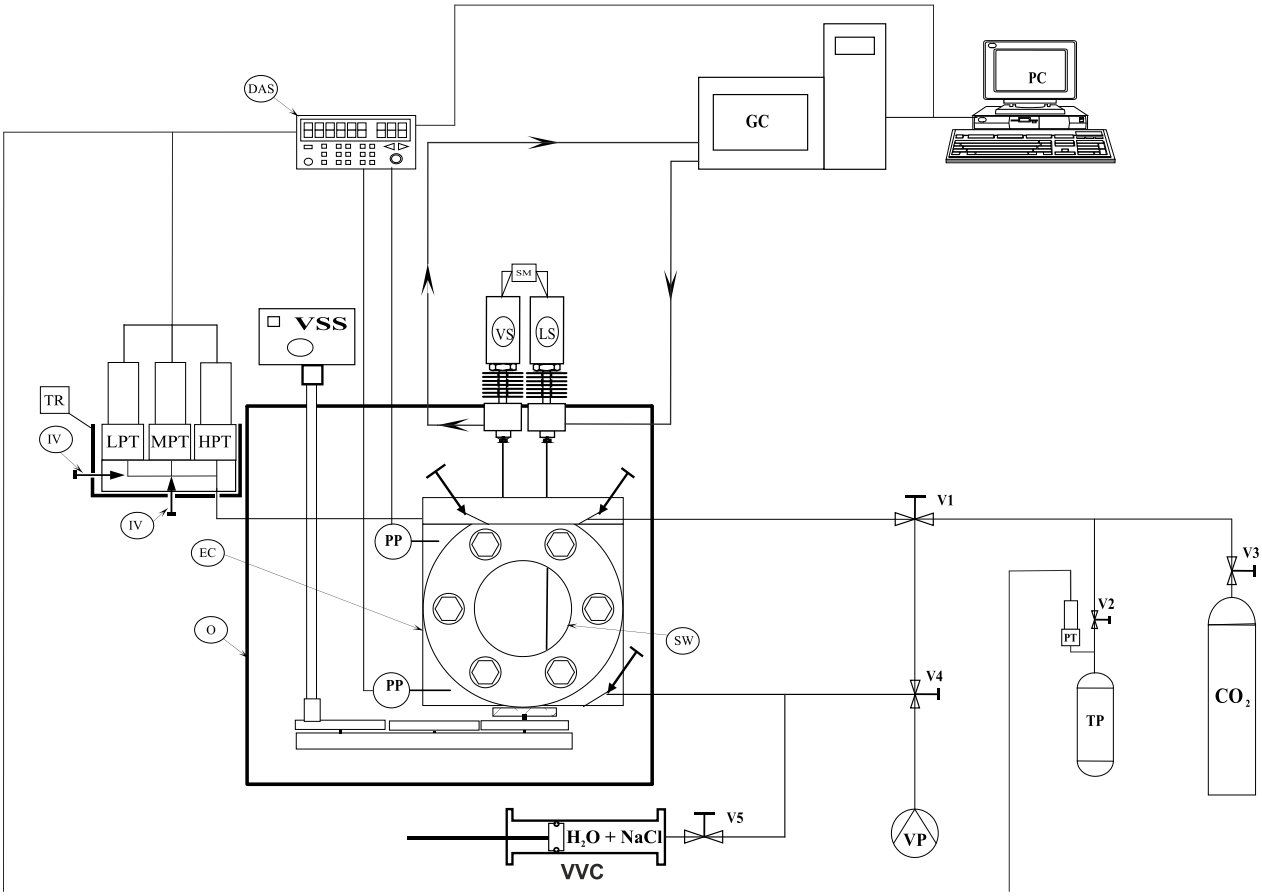


Figure 1 : Schematic representation of the apparatus for measuring the solubility of CO_2 in NaCl brine. DAS: data acquisition system, EC: equilibrium cell, GC: gas chromatography, HPT: high pressure transducer, LPT: low pressure transducer, LS: liquid ROLSI® Sampler-Injector, MPT: medium pressure transducer, O: oven, PP: platinum resistance thermometer probe, PT: pressure transducer, IV: homemade shut off valve, SM: samplers monitoring, SW: sapphire window, TP: thermal press, TR: temperature regulator, Vi: valve i, VP: vacuum pump, VS: vapor ROLSI® Sampler-Injector, VSS: variable speed stirrer and VVC: Variable Volume Cell.

2.1. Materials

In Table 1, we list the suppliers of the two chemicals and the purities (given by the suppliers). Carbon dioxide (CO_2, CAS Number: 124-38-9) was purchased from Messer with a certified volume purity greater than 99.995%. Sodium chloride (NaCl, CAS Number: 7647-14-5) was purchased from Fisher Chemical with a certified purity of 99.6%.Water was deionized and degassed before the preparation of the brine (water + NaCl).

Table 1 : Purities and suppliers of the chemicals used in this work

Chemicals	Purity	Analytical Method	Supplier
CO_2	99.995 vol%	Gas Chromatography	MESSER
NaCl	99.6%	None	Fisher Chemical

2.2. Apparatus description

Figure 1 illustrates the experimental set-up for the measurement of CO_2 solubility in brine. The principle of this apparatus is similar to that described by El Ahmar et al. [16], and is based on the "static-analytic" method. It consists of an Equilibrium Cell (EC) with a volume of 235 cm^3, with two Sapphire Windows (SW), and positioned in an Oven (O) to maintain a constant temperature. The equilibrium cell is equipped with three pressure transducers for Low (LPT), Medium (MPT) and High (HPT) pressure, two Platinum resistance thermometer Probes (PP) and two ROLSI® (Rapid On-Line Sampler-Injector, French patent number 0304073) capillary samplers, one for the vapor phase and the other for the liquid phase. The LPT and MPT pressure transducers are isolated at 30 and 100 bar respectively using the home made shut off Valve (IV). The signals received by the Data Acquisition System (DAS) from pressure transducers and temperature probes are processed by the PC via the LTC10 interface. The feeding of the equilibrium cell by the saline solution (water + NaCl) is done by a Variable Volume Cell (VVC). Depending on the desired pressure, CO_2 is introduced either directly from the cylinder or from the Thermal Press (TP) for higher pressures. The system is agitated by a Variable Speed Stirrer (VSS). Samples are analyzed by a gas chromatograph (Shimadzu GC-2014) equipped with a Thermal Conductivity Detector (TCD) to capture CO_2 and water signals. The transfer line between the ROLSI® and the GC is overheated in order to avoid salt deposition on the ROLSI® mobile part, as well as a pre-column has been added to protect the separation column. The packed column used for the separation of CO_2 and water is Porapak Q, 80/100 mesh, 2m×1/8 in. Silcosteel (Restek, France).

2.3. Calibrations

Due to the large volume of the equilibrium cell, the temperature is measured at two locations (top and bottom of the cell) in order to know the precise temperature of the equilibrium cell and to check the thermal gradients. These temperature measurements are carried out by two platinum

resistance thermometers (100 Ω), which are calibrated against a 25-Ohm platinum resistance thermometer (model 5628, Fluke (Hart Scientific)) combined with an Agilent 34420A precision Ohmmeter, and calibrated by LNE (Laboratoire National de Métrologie et d'Essais). The calibration accuracies of the temperature probes at the top and bottom of the equilibrium cell are not higher than ±0.008 K and ±0.007 K respectively, and are composed of two contributions: the uncertainty related to the standard probe and the uncertainty related to the polynomial equation established between the values transmitted by the probes and the values of the standard probe. The LPT, MPT and HPT pressure transducers were calibrated against pressure automated calibration equipment (PACE 5000, GE Sensing and Inspection Technologies). Above 100 bar, the HPT pressure transducer was calibrated against a dead weight pressure balance (Desgranges & Huot 5202S, CP 0.3–40MPa, Aubervilliers, France). The calibration accuracies of the LPT, MPT and HPT transducers are calculated in the same way as those of the temperature probes and are equal to ±0.2 kPa, ±0.2 kPa and ±0.3 kPa, respectively. The saline solution (water + NaCl) was prepared gravimetrically using a mass comparator (CC1200, Mettler-Toledo) with an uncertainty of 1 mg. Calibration of the thermal conductivity detector (TCD) was done by introducing and analyzing known quantities of compounds (water and CO_2) using suitable syringes. The calibration accuracy of the TCD is less than ±1.3% on the mole number of CO_2 and less than ±1.6% on the mole number of water, and it consists of the uncertainty associated with injection by syringe and the accuracy related to the polynomial equation established between the specific area of the peak obtained (S_1) and the number of moles (n_1). The uncertainty related to the repeatability of measurements is the most important, especially for solubility (xCO_2). The total uncertainties on temperature, pressure and composition, including all sources of error (calibration and repeatability) are reported in Table 2.

2.4. Experimental procedure and results

For each measured point, the following procedure was followed: setting the target temperature, evacuating the loading lines and the equilibrium cell and introducing the saline solution through the variable volume cell until approximately one third of the cell was filled. Then, the CO_2 is introduced from the top of the cell until the desired pressure is reached. Stirring is started and thermodynamic equilibrium is reached in a few minutes. Once, the pressure and temperature are stabilized, several samples are taken from the liquid phase by the ROLSI® capillary sampler and

sent via the transfer line to the GC for analysis. The data are processed by deducting the mole number n_i of each component i (water or CO_2) from the surface of the corresponding peak. Then, the salt-free molar fraction $x_{CO_2}^{sf}$ of CO_2 is determined as follows:

$$x_{CO_2}^{sf} = \frac{n_{CO_2}}{n_{CO_2} + n_{H_2O}} \quad (1)$$

The true mole number can be obtained from the following expressions:

$$x_{CO_2} = \frac{n_{CO_2}}{n_{CO_2} + n_{H_2O} + m_s \cdot n_{H_2O} \cdot M_{H_2O}} \quad (2)$$

Because $n_{salt} = m_s \cdot n_{H_2O} \cdot M_{H_2O}$

where m_s is the NaCl molality and M_{H_2O} is the molar mass of water.

Consequently

$$x_{CO_2} = \frac{x_{CO_2}^{sf}}{x_{CO_2}^{sf} + \left(1 - x_{CO_2}^{sf}\right)\left(1 + m_s \cdot M_{H_2O}\right)} \quad (3)$$

The very small quantities withdrawn during sampling do not modify the thermodynamic equilibrium. Since some water is evaporated, there is no significant increase of the salt molality of the solution, therefore the molality of the solution has been considered constant. Another equilibrium point is measured by adding more CO_2 and so on until the desired maximum pressure is reached. Before starting a new isotherm or introducing a solution with a different molality than the one before, the equilibrium cell is cleaned and evacuated.

The experimental measurements were performed at molalities between 1 and 3 m, temperatures between 50 and 100°C and pressures up to 230 bar, and are listed in Table 2. The number of points measured for each isotherm is different because of some difficulties encountered such as the clogging of the ROLSI® capillary sampler by salt deposit or leaks in the circuit, which requires the shutdown and maintenance of the apparatus.

Table 2 : Experimental and calculated solubilities of carbon dioxide in the CO_2 + H_2O + NaCl system, expressed as "salt-free" mole fractions.

	Experimental data				calculation							
					m-SW model		e-PR-CPA model		Geoch. model		DUAN model	
m_{NaCl} (mol/kg_w)	T (K)	P (bar)	$x_{CO_2}^{sf}$	$u(x_{CO_2}^{sf})$ [a]	$x_{CO_2}^{sf}$	AD % [b]	$x_{CO_2}^{sf}$	AD % [b]	$x_{CO_2}^{sf}$	AD % [b]	$x_{CO_2}^{sf}$	AD % [b]
1.13	372.33	31.148	0.00390	2.0E-04	0.00414	6.08	0.00418	7.14	0.00435	11.67	0.00445	14.19
	372.31	60.500	0.00750	2.0E-04	0.00755	0.73	0.00755	0.70	0.00776	3.46	0.00784	4.48
	372.29	108.840	0.01130	2.5E-04	0.01190	5.34	0.01174	3.91	0.01190	5.31	0.01183	4.70
	372.29	151.920	0.01360	3.5E-04	0.01461	7.45	0.01428	5.00	0.01442	6.06	0.01411	3.75
	372.25	191.980	0.01570	6.0E-04	0.01644	4.73	0.01595	1.61	0.01614	2.79	0.01550	1.29
1.13	323.02	53.450	0.01030	3.0E-04	0.01088	5.59	0.01122	8.95	0.01130	9.72	0.01145	11.18
	322.97	75.550	0.01290	3.0E-04	0.01384	7.32	0.01414	9.61	0.01402	8.67	0.01418	9.95
	323.03	100.350	0.01510	7.5E-04	0.01591	5.36	0.01611	6.70	0.01586	5.04	0.01618	7.16
	323.04	145.080	0.01700	4.5E-04	0.01756	3.28	0.01761	3.60	0.01740	2.33	0.01709	0.54
1.00	373.38	16.983	0.00237	1.0E-04	0.00230	3.07	0.00233	1.72	0.00247	4.05	0.00254	6.96
	373.37	32.527	0.00426	2.0E-04	0.00436	2.56	0.00440	3.30	0.00461	8.25	0.00470	10.49
	373.41	68.182	0.00833	2.0E-04	0.00847	1.70	0.00843	1.26	0.00869	4.30	0.00874	4.97
3.01	342.82	30.391	0.00441	1.0E-04	0.00405	8.18	0.00421	4.62	0.00398	9.83	0.00419	4.99
	342.81	72.559	0.00880	2.0E-04	0.00829	5.83	0.00840	4.53	0.00793	9.91	0.00811	7.88
	342.82	100.910	0.01057	3.0E-04	0.01021	3.44	0.01023	3.24	0.00968	8.38	0.00978	7.43
3.01	372.39	25.556	0.00292	8.0E-05	0.00264	9.44	0.00276	5.46	0.00261	10.58	0.00277	5.10
	372.42	71.417	0.00707	1.5E-04	0.00661	6.46	0.00676	4.41	0.00643	9.06	0.00654	7.49
	372.41	100.517	0.00878	3.0E-04	0.00854	2.71	0.00864	1.58	0.00825	5.99	0.00826	5.93

372.43	152.433	0.01141	2.5E-04	0.01102	3.42	0.01100	3.55	0.01063	6.86	0.01034	9.35
372.45	199.597	0.01258	3.0E-04	0.01254	0.32	0.01242	1.23	0.01214	3.51	0.01152	8.42
372.45	229.817	0.01337	3.0E-04	0.01330	0.52	0.01312	1.81	0.01292	3.34	0.01215	9.09
AAD %					**4.45**		**4.00**		**6.62**		**6.92**

[a] u: standard uncertainties, $u(T) = 0.02\ K$ and $u(P) = 5\ kPa$. [b] AD %: absolute deviation, AD % $= 100 \cdot \left| \frac{x_{CO_2}^{cal} - x_{CO_2}^{exp}}{x_{CO_2}^{exp}} \right|$, AAD %: average absolute deviation, AAD % $= \frac{100}{N_{exp}} \sum_{i=1}^{N_{exp}} \left(\left| \frac{x_{CO_2\,i}^{cal} - x_{CO_2\,i}^{exp}}{x_{CO_2\,i}^{exp}} \right| \right)$.

3. Thermodynamic modeling

3.1. Soreide and Whitson EoS

The first thermodynamic model used in this work is the cubic Equation of State (EoS) proposed by Soreide and Whitson [3], which is a revised form of the well-known Peng-Robinson EoS (PR-EoS) [17]. The Soreide-Whitson model is widely used in the oil and gas field especially for systems in the presence of water or brine, and is implemented in several modeling software like reservoir simulators such as Eclipse 300 (by Schlumberger), IHRRS (by Total) and IPM (by Petex), and thermophysical properties calculators like Simulis Thermodynamics (by Prosim), etc.

To describe the phase equilibria of gas-water and gas-brine systems, Soreide and Whitson (SW) proposed two modifications to the PR-EoS. The expression of the equation of state (PR EoS) remains the same, while the alpha function and the mixing rules were modified (see Appendix A). This last modification concerns the use of two different binary interaction coefficients (k_{ij}), one for the aqueous phase k_{ij}^{AQ} and the other for the non-aqueous (gas-rich) phase k_{ij}^{NA}. These two parameters are respectively adjusted on gas solubility data and water content data of gas-water-NaCl systems. The k_{ij}^{NA} is generally constant or slightly dependant on temperature, however, the k_{ij}^{AQ} depends on temperature and molality.

It should be noted that the use of two different k_{ij} makes the model inconsistent (which makes it equivalent to a gamma-phi approach), this limitation is effective especially near to the critical points region of the system (which is above 265 °C according to Todheide and Franck [5]), and does not really represent a problem for reservoir simulation since the maximum temperature in geological formations is about 150 °C. The problem of inconsistency that may occur is on the implementation of the model in the simulators knowing that in the original model, salinity is considered static, therefore it is not taken into account in the derivative of the attractive term a, whereas it must be considered dynamic.

$$\left.\frac{\partial a}{\partial n_{w,w}}\right|^{dynamic} = \left.\frac{\partial a}{\partial n_{w,w}}\right|^{static} - \left.\frac{\partial a}{\partial m_s}\right|_{n_{j,w}} \left.\frac{\partial m_s}{\partial n_{w,w}}\right|_{n_{j\neq i,w}} \tag{4}$$

Petitfrere et al. [18] considered a dynamic salinity (Eq. (4), for more details see the original paper [18]) and proposed some modifications to the implementation of the SW model to make it consistent and compared it to the original implementation by the simulation of CO_2 injection process in a saline aquifer with their simulation software (IHRRS). They showed

that the simulation results are not sensitive to this inconsistency problem; the most important thing is the correct prediction of mutual solubilities. But it is preferable to implement this model according to the approach they proposed in order to be able to do the stability analysis (to know if there is a phase split in each cell and also to initialize the flash calculations).

Yan et al. [7] showed that the Soreide and Whitson model underestimates the solubility of carbon dioxide at high molalities, and they proposed a better correlation for $k_{CO_2,w}^{AQ}$ by refitting it to solubility data of CO_2 in water and NaCl brine. Soreide and Whitson [3] and Yan et al. [7] included only the experimental data of water content of the CO_2-H_2O system to adjust the binary interaction parameters, and they did not include the experimental data of water content for the CO_2-H_2O-NaCl system since they did not exist until 2013. The phase equilibria (liquid and vapor phase) for this system were recently measured by Hou et al. [8]. In this work these data were added to our database and used to adjust the binary interaction parameters $k_{CO_2,w}^{NA}$ and $k_{CO_2,w}^{AQ}$. The new expressions for these parameters are given by

$$\left(k_{CO_2,w}^{NA}\right)_{New} = 0.68208385571 \cdot 10^{-3}T - 2.066623464504 \cdot 10^{-2} \tag{5}$$

$$\left(k_{CO_2,w}^{AQ}\right)_{New} = \left(\frac{T}{T_{c,CO_2}}\right)\left[a + b\left(\frac{T}{T_{c,CO_2}}\right) + c\left(\frac{T}{T_{c,CO_2}}\right)m_s\right] + m_s^2\left[d + e\left(\frac{T}{T_{c,CO_2}}\right)\right] + f \tag{6}$$

where T is the temperature in K, and $T_{c,CO_2} = 304.13$ K is the CO_2 critical temperature. Coefficients a, b, c, d, e and f are listed in Table 3. For $k_{CO_2,w}^{NA}$, temperature dependence has been added since it has been observed that $k_{CO_2,w}^{NA}$ varies slightly with a linear trend with respect to temperature and this modification improves the representation of the water content (decrease of AAD(y_w) by 1.5%). In this work, the Soreide and Whitson model with the new parameters is called m-SW.

Table 3 : Coefficients of the $\left(k_{CO_2,w}^{AQ}\right)_{New}$ correlation (Eq. (6))

a	0.43575155
b	$-5.766906744 \cdot 10^{-2}$
c	$8.26464849 \cdot 10^{-3}$
d	$1.29539193 \cdot 10^{-3}$
e	$-1.6698848 \cdot 10^{-3}$
f	-0.47866096

3.2. e-PR-CPA EoS

The second thermodynamic model developed in this work is the e-PR-CPA (electrolyte Peng-Robinson Cubic Plus Association EoS). The idea of CPA (Cubic Plus Association) EoS [19] is to present the contribution of intermolecular interactions between molecules with a cubic equation of state (Peng-Robinson (PR) or Soave-Redlich-Kwong (SRK) [20]) and to add the Wertheim associative term [21] in order to take into account the association phenomenon (hydrogen bonding in solutions). For the cubic term, the PR (1978) EoS [22] was chosen in the continuity of previous work (Hajiw el al. 2015 [23] and Wang et al. 2018 [24, 25]) and because it better represents liquid density [17] by comparing it with the SRK EoS.

The representation of electrostatic forces (long range interactions) can be done by one of the two theories: the complete Debye-Huckel theory (DH) used by the Sadowski [26], Kontogeorgis [27] groups, etc. and which treats ions as point charges; the Mean Spherical Approximation (MSA) theory which is used by various research groups (Jackson [28], De Hemptinne [29], Fürst [30], etc.) and which considers ions as charged hard spheres. A very good comparison of the two theories was made by Maribo-Mogensen et al. [31] shows that numerically the two theories behave in a very similar way. They also showed that only MSA correctly predicts the increase in screening length by increasing the ion diameter, since in DH the screening length is independent of the diameter. In this work we have chosen the MSA theory.

The electrolyte contribution in the e-PR-CPA model is represented by two terms: the first term comes from the MSA theory [32] for the representation of ion-ion long range interactions and the second term is the Born term [33] for the representation of short range interactions between solvent and ions (solvation).

The expression for the residual Helmholtz free energy of the e-PR-CPA model is as follows:

$$\frac{A^{res}_{e-PR-CPA}}{RT} = \frac{A^{PR}}{RT} + \frac{A^{Association}}{RT} + \frac{A^{MSA}}{RT} + \frac{A^{Born}}{RT} \tag{7}$$

The non-electrolyte part of this model consists of two terms. Repulsive and attractive interactions are taken into account with the term $\frac{A^{PR}}{RT}$ of the PR EoS. The association phenomenon (self-association and cross-association) are represented by the term $\frac{A^{Association}}{RT}$ from Wertheim's theory. The different terms of equation 6 are detailed in Appendix B.

The diameters σ_i of ions i used in the Born term and in the MSA term (see Appendix B) are the same as the ones used to calculate the co-volume of the ions b_{ion}. In this work, we neglect the formation of ion pairs, that occur at very high temperatures (above 300°C) [34]. The temperature in geological reservoirs, salt caverns and saline aquifers are generally not higher than 200°C [35], so we can assume that NaCl is fully dissociated in the solution.

Parameterization of the e-PR-CPA model

The parameterization of the e-PR-CPA model consists of determining the five parameters (m_i, $a_{0,i}$, b_i, ε_i, β_i) of pure water and three parameters (m_{ion}, $a_{0,ion}$, σ_{ion}) for each ion. The adjustment of the parameters was carried out by a hybrid optimization program (simulated annealing combined with BFGS [36]) by minimizing the following objective function:

$$F_{obj} = \frac{100}{N}\sum_{i=1}^{N}\left(\left|\frac{val_i^{cal} - val_i^{exp}}{val_i^{exp}}\right|\right) \quad (8)$$

where N represents the number of data, val corresponds to the thermodynamic property calculated by the model (cal) or measured experimentally (exp).

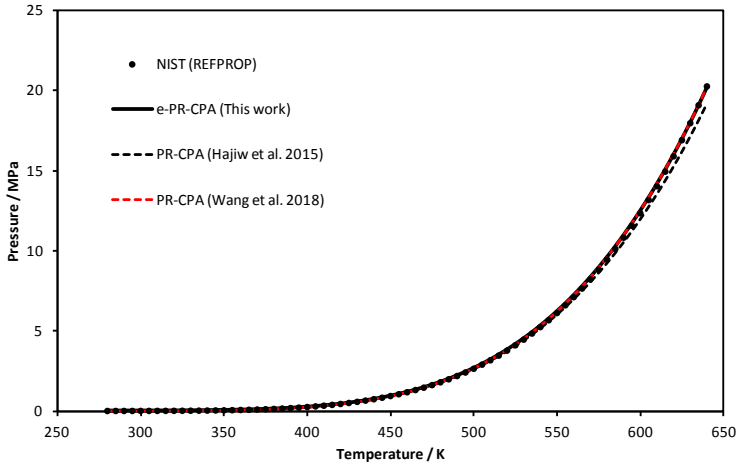
- Pure water

According to the terminology of Huang and Radosz [37], the 4C association scheme with two electron donor sites and two electron acceptor sites has been applied in this work to describe water molecule. The parameters (m_i, $a_{0,i}$, b_i, ε_i, β_i) for pure water are obtained by adjusting to vapor pressure and saturated liquid density data correlated by NIST [38]. The water parameters obtained in this work and those obtained previously by Hajiw et al. [23] and Wang et al. [24, 25] are reported in Table 4. As shown in Figure 2, the e-PR-CPA model can accurately describe the pure water VLE data, apart in the near critical region.

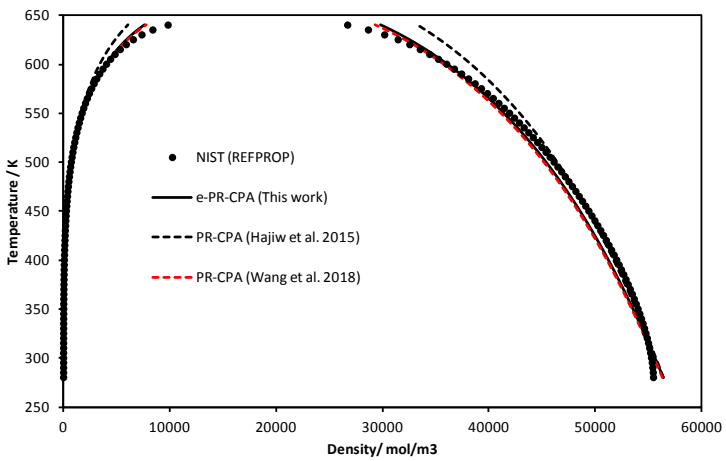
Table 4 : Pure water parameters (e-PR-CPA model), comparison with parameters from Hajiw et al. [23] and parameters from Wang et al. [24].

Water (4C)								
	m	a0 ($Pa.m^2/mol^2$)	b (m^3/mol)	ε ($Pa.m^3/mol$)	β	Range of Tr	AAD % [a]	
							P_{sat}	ρ_{liq}
Hajiw et al. 2015	0.6387	0.2174	1.52E-05	14639	6.83E-02	0.43-0.99	**1.04**	**2.46**
Wang et al. 2018	0.6740	0.1230	1.44E-05	17048	6.98E-02	0.43-0.99	**1.11**	**1.74**
This work	0.6755	0.1323	1.45E-05	16823	6.91E-02	0.43-0.99	**1.12**	**1.51**

[a] $AAD\% = \frac{100}{N}\sum_{i=1}^{N}\left(\left|\frac{val_i^{cal} - val_i^{exp}}{val_i^{exp}}\right|\right)$, val : P_{sat} or ρ_{liq}



a



b

Figure 2 : Comparison of the e-PR-CPA model (with the three parameter sets in Table 4) with the NIST model. a) Water vapor pressure, b) Water density at saturation.

Over the entire temperature range, the parameters obtained in this work and those obtained by Wang et al. give the best results in terms of vapor pressure and density. It appears that the parameters of Hajiw et al. have been adjusted to the temperature range of the application of interest; however they better estimate the vapor pressure and density at temperatures below 500K. The third set of parameters (obtained in this work, Table 4) was chosen for the rest of the work.

- H_2O + NaCl system

There are three parameters ($m_{ion}, a_{0,ion}, \sigma_{ion}$) specific to each ion ($Na^+$ and Cl^-). To represent both the equilibrium properties and the excess properties, we have decided to adjust these parameters on saturation vapor pressure data and on osmotic coefficient data of the water + NaCl system. No binary interaction parameters were used for this system ($k_{Na^+-Cl^-} = k_{water-Na^+} = k_{water-Cl^-} = 0$). The optimized ion parameters and the results obtained by the e-PR-CPA model are shown in Table 5 and Figure 3-5 respectively.

Table 5 : The parameters of the Na^+ and Cl^- ions (e-PR-CPA model).

	m	a_0 (Pa.m^2/mol^2)	σ (Å)
Na^+	-1.5684	1.15236	1.0945
Cl^-	0.2489	0.93705	3.6391

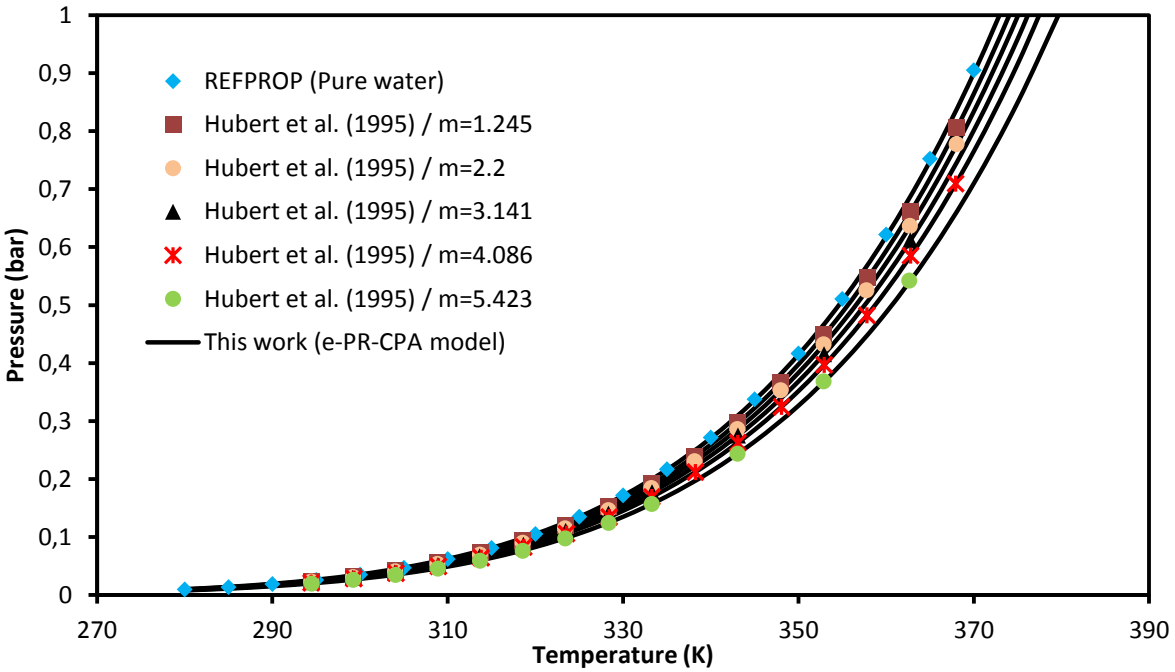


Figure 3 : Saturation vapor pressure of water + NaCl at low temperature and at different NaCl molalities. Comparison of the e-PR-CPA model with the experimental data of Hubert et al. [39].

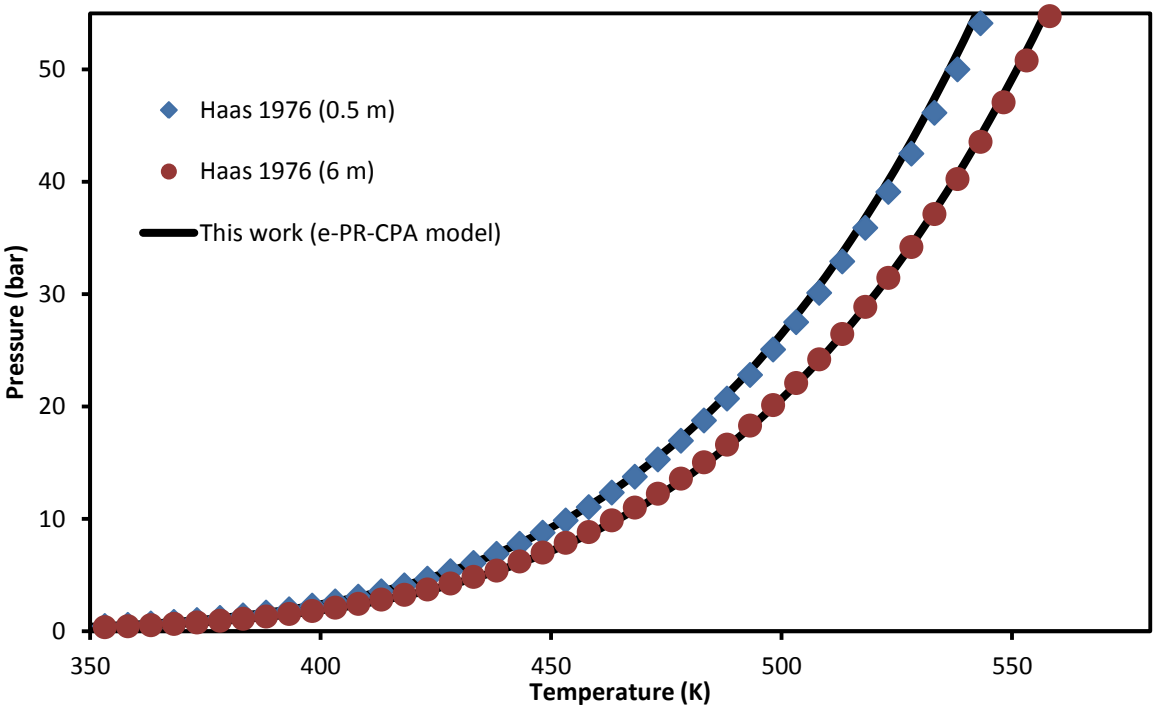


Figure 4 : Saturation vapor pressure of water + NaCl at high temperature and at 0.5 and 6 moles/kgw of NaCl. Comparison of the e-PR-CPA model with the data correlated by Hass [40].

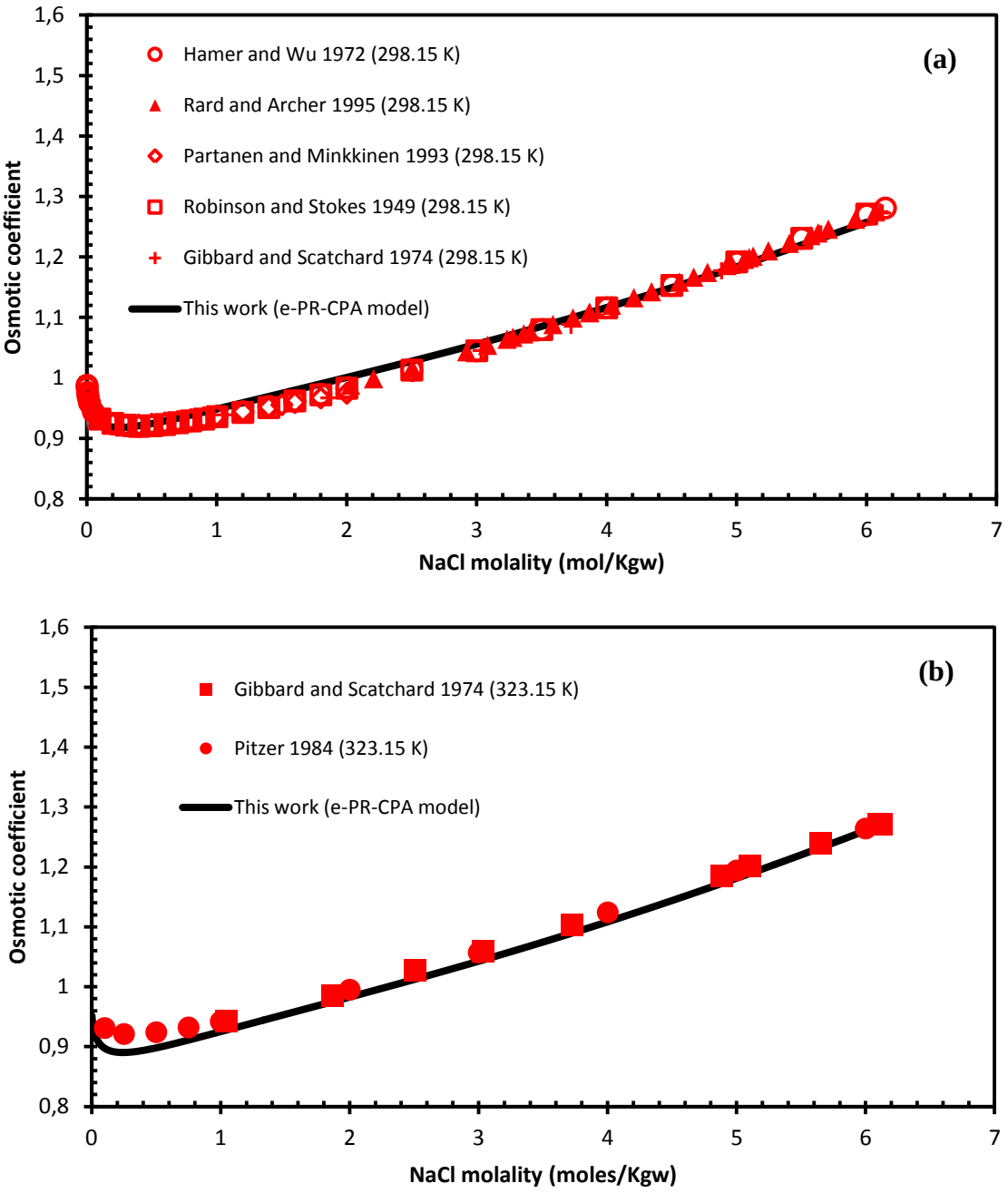


Figure 5 : Osmotic coefficient of water + NaCl versus NaCl molality at 298.15 K (a) and 323.15 K (b). Comparison of the results of the e-PR-CPA model with the experimental data from [41-46].

The AAD of the vapor pressures and osmotic coefficients of the H_2O-NaCl system calculated for temperatures up to 300°C and molalities up to 6m NaCl are shown in Table 6 and are reproduced within an AAD of 1.87% and 2.02% respectively.

Table 6 : AAD (%) of the vapor pressure and osmotic coefficient calculated with the e-PR-CPA model.

	Number of data	Range of T (K)	Maximal Molality	AAD (%)	References
Vapor pressure	448	294 - 573	6	1.87	[39, 40]
Osmotic coefficient	196	298 - 573	6.24	2.02	[41-46]

3.3. Geochemical model

The third model tested in this work is a geochemical model implemented in CHESS/HYTEC software (Corvisier, 2013 [13]; Corvisier et al., 2013 [14]). It implies a dissymmetrical approach $\gamma - \varphi$:

$$m_i^{aq}\gamma_i^{aq}\mathrm{K}_i^g(T,P^{sat})\exp\left(v_i^{\infty}\frac{P-P^{sat}}{RT}\right) = \mathrm{y}_i^g\varphi_i^g P \qquad (9)$$

where m_i^{aq} is the molality (mol/kg of water) of the dissolved gaseous component i, γ_i^{aq} its activity coefficient, K_i^g the Henry's law constant at water saturation pressure, v_i^{∞} the molar volume of the dissolved gaseous component at infinite dilution, y_i^g the component mole fraction in the gas phase and φ_i^g its fugacity coefficient.

Let us recall that this model uses an important database and could solve a large set of mass balances and mass action laws to calculate the whole system speciation (i.e. pH, concentrations of species such as HCO_3^-, CO_3^{2-}, $NaCO_3^-$..., potential minerals dissolution/precipitation). It is also important that equations remain generic, in order that the model remains multi-component either for the gas phase and the electrolyte.

For the gas phase, the PR-SW EoS is then used with the classical mixing rule.

Aqueous activity coefficients can be calculated using various models, but as far as saline solutions with high ionic strength are concerned, specific models should be used, as for example the well-known Pitzer model (Pitzer 1973 [47], Pitzer 1991 [48]). The Specific Ion Theory model (SIT) already implemented in CHESS/HYTEC software is simpler and allows obtaining satisfactory results on such systems. SIT theory first mentioned by Bronsted (Bronsted 1922) [49] and later by Scatchard (Scatchard 1936 [50]) and Guggenheim (Guggenheim & Turgeon 1955 [51]) takes short-distance forces into account by adding terms

to the Debye-Hückel law (Debye & Hückel 1923 [52]). The theoretical details of this approach are explained in Grenthe's work (Grenthe & Puigdomenech 1997 [53]). The fundamental equation of the SIT model is given by:

$$ln(\gamma_i^{aq}) = \frac{-Az_i{}^2\sqrt{I}}{1 + 1.5\sqrt{I}} + \sum_j m_j^{aq}\,\varepsilon_{ij} \quad (10)$$

where A the first Debye-Hückel parameter (function of the temperature), I the ionic strength of the solution, z_i the charge of the aqueous species i, and ε_{ij} binary interaction parameters between aqueous species i and j.

Best Henry's law constant, molar volume for its pressure correction and gas binary interaction parameters for CO_2 have been selected from the literature or fitted in a previous work (Hajiw et al. 2018 [54]). Aqueous binary interaction parameters for the SIT model have been fitted on experimental data.

- $\varepsilon_{H^+Cl^-}$ and $\varepsilon_{Na^+Cl^-}$ are equal to -0.062 and -0.021 respectively, using HCl and NaCl solutions activity measurements (Schneider et al. 2004 [55], Sakaida & Kakiuchi 2011 [56], Khoshkbarchi & J.H. Vera 1996 [57])
- $\varepsilon_{CO_2Na^+}$ varying with temperature (from 0.261 at 25°C to -0.624 at 200°C), using numerous CO_2 solubility measurements in NaCl solutions.

4. Results and discussions

4.1. $H_2O + CO_2$ binary system

The molecular representations of carbon dioxide and water with the association sites assigned to each of these molecules are shown in Figure 6. For the H_2O-CO_2 binary system, solvation was considered by assuming that CO_2 has only one electron acceptor (ea) site (type 0ed-1ea) and that H_2O has 4 association sites (type 4C) with two electron donor (ed) sites and two electron acceptor sites. However, the modified combining rules m-CR1 (Eq. (35-36)) are used.

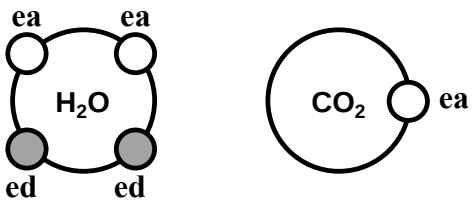


Figure 6 : Molecular representations of water and carbon dioxide in terms of electron donor/acceptor sites. ed: electron donor site, ea: electron acceptor site

In order to investigate the influence of the temperature, the binary interaction parameter $k_{H_2O-CO_2}$ and the cross association volume $\beta_{H_2O-CO_2}$ of the H_2O-CO_2 binary system were optimized on solubility data (Wiebe and Gaddy 1939 [58], Yan et al. 2011 [7] and Hou et al. 2013 [59]) simultaneously for each temperature (in the range of 323 - 423 K). Figure 7 shows the trend of these two parameters with respect to temperature. To reproduce this trend, a 1st degree (Eq. (11)) and 2nd degree (Eq. (12)) polynomial equations have been proposed for $k_{H_2O-CO_2}$ and $\beta_{H_2O-CO_2}$ respectively.

$$k_{H_2O-CO_2} = 1.522403212 \cdot 10^{-3} T - 0.339526533 \quad (11)$$

$$\beta_{H_2O-CO_2} = 6.982115486 \cdot 10^{-6} T^2 - 4.334449524 \cdot 10^{-3} T + 0.849767346 \quad (12)$$

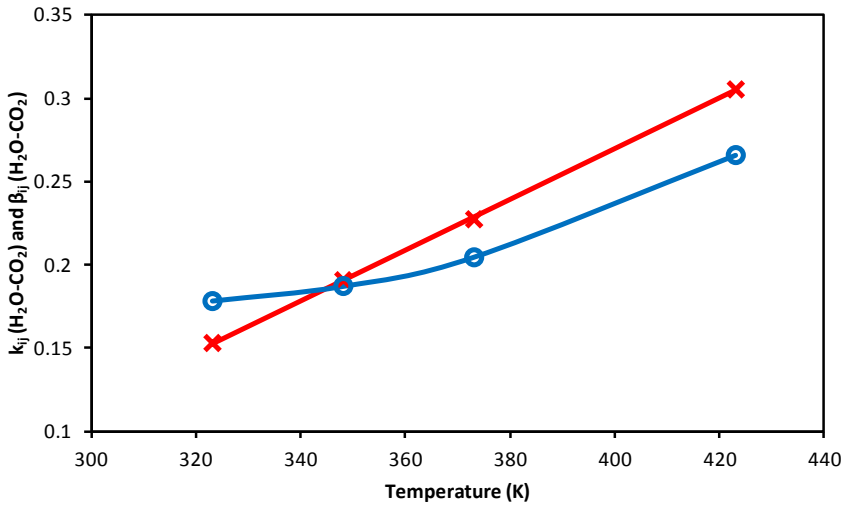


Figure 7 : Influence of temperature on $k_{H_2O-CO_2}$ (×) and on $\beta_{H_2O-CO_2}$ (o) for the H_2O-CO_2 system. Symbols represent optimized parameter values; solid lines represent correlations (Eq. (38-39)).

The CO_2 solubility in water and water content of the H_2O-CO_2 system are shown in Figure 8. The symbols represent the experimental data and the lines (solid, dotted and dashed) represent the calculations done by the e-PR-CPA, Geochemical and m-SW models, respectively. The predictions (calculations outside the adjustment range) of CO_2 solubility and water content at 298.15 K with the e-PR-CPA model are shown in Figure 8-c and 8-d and are compared with the calculations obtained by the m-SW and the geochemical models. The three models can accurately describe the CO_2 solubility in water and the water content. The CO_2 solubility in water is better represented with the e-PR-CPA model. However, the geochemical model and the m-SW model give slightly better results for the calculation of the water content since for the later two different binary interaction coefficients are used for each phase.

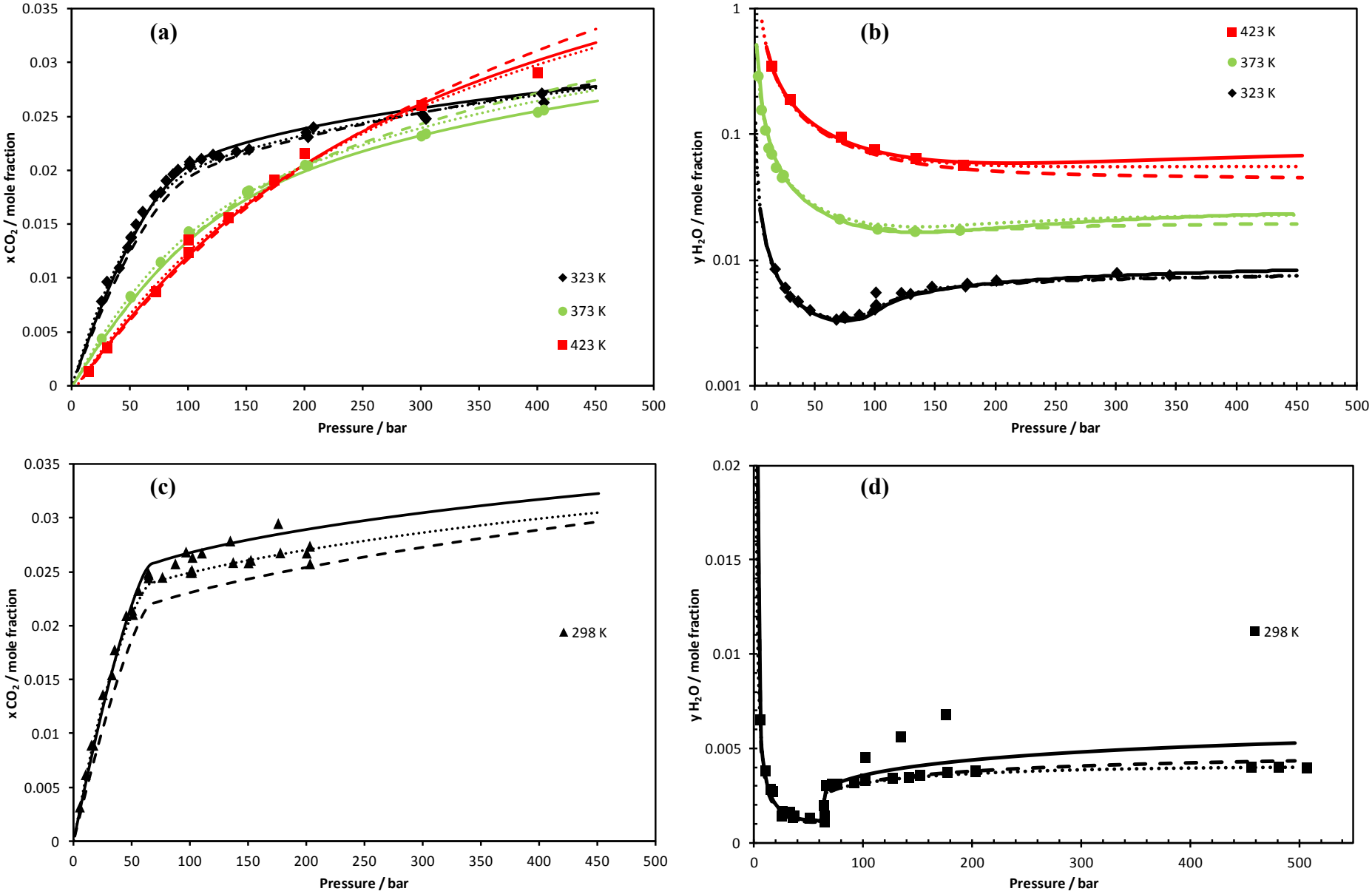


Figure 8 : CO_2-H_2O binary system: Calculation of CO_2 solubility in water (a and c) and water content (b and d) at 298, 323, 373 and 423 K by e-PR-CPA (solid line), m-SW (dashed line) and geochemical (dotted line) models. The symbols are literature data: (a): [6, 7, 58-62], (b): [59, 61, 63-66], (c): [59, 67-71], and (d): [59, 67-70, 72].

4.2. Prediction of the phase equilibria of the CO_2-H_2O system at very high pressure and temperature.

The ability to extrapolate the e-PR-CPA model outside the adjustment range was investigated by predicting the liquid-vapor equilibria of the CO_2-H_2O system at very high pressures (up to 3000 bar) and temperatures (up to 573 K). This binary system is classified as type III according to Scott and van Konynenburg [73] classification. The Predictions of the e-PR-CPA model compared with experimental data from the literature are shown in Figure 9. There is a mixture critical point at 548 K and 573 K. In all pressure/temperature ranges, the solubilities of carbon dioxide in water and water content are well estimated. Note that the experimental data for the vapor phase at 473 K are not consistent, and the model predictions are between two independent sets of experimental data (Todheide and Franck [5] and Takenouchi and Kennedy [6]).

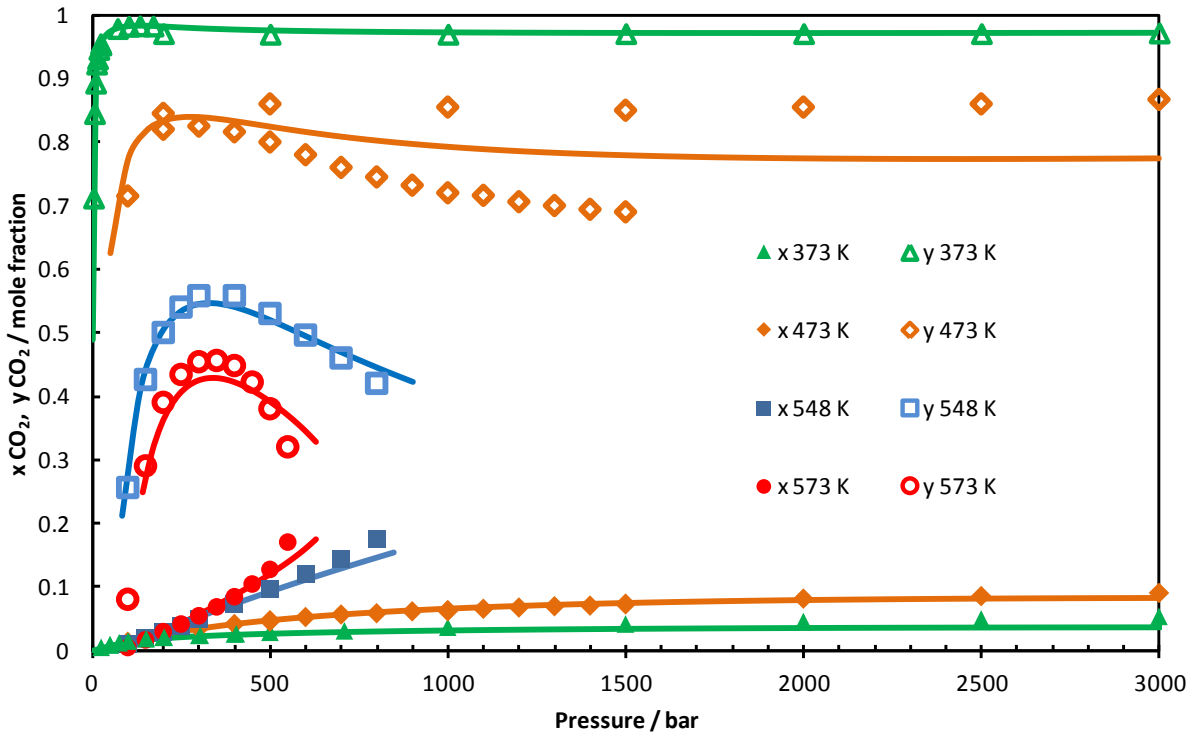


Figure 9 : CO_2-H_2O system: Prediction of liquid-vapor equilibria at very high temperature and pressure by the e-PR-CPA model. The symbols are literature data: [5, 6].

4.3. H_2O + CO_2 + NaCl system

In Figure 10, the calculation results of the solubility of CO_2 in high molality NaCl brine (4m and 6m) by the Soreide and Whitson (SW) model were presented using two sets of binary interaction parameters (BIPs): the original BIPs and the BIPs proposed in this work (m-SW).

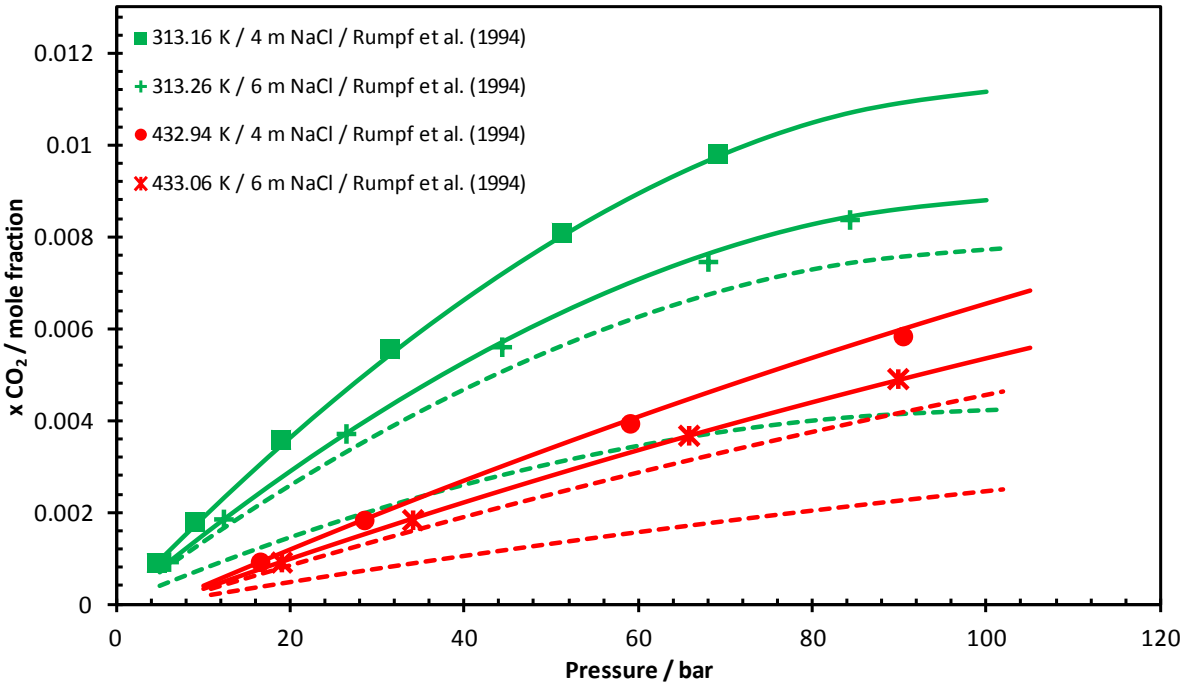


Figure 10 : CO_2-H_2O-NaCl system: Calculation of CO_2 solubility in high molality NaCl brine at 313 K and at 433 K by the Soreide and Whitson (SW) model using the original kij (dashed line) and the kij proposed in this work (solid line). Literature data from Rumpf et al. [74].

Comparing these results with literature data, a significant improvement was made with the new BIPs (m-SW), especially at high molality.

The description of phase equilibria in the presence of electrolytes with the e-PR-CPA model requires the introduction of binary interaction parameters $k_{gas-ions}$ between CO_2 and the ions (Na^+ and Cl^-). These parameters ($k_{CO_2-Na^+}$ and $k_{CO_2-Cl^-}$) are obtained by adjusting the model parameters to solubility data (Rumpf et al. 1994 [74], Koschel et al. 2003 [4] and Yan et al. 2011 [7]) of carbon dioxide in brine (H_2O + NaCl). To be in good agreement with the experimental data, we noticed that the $k_{gas-ions}$ are slightly dependent on molality (Figure 11). Since, the effect of temperature is already taken into account in $k_{H_2O-CO_2}$ and $\beta_{H_2O-CO_2}$, a simple linear dependence of $k_{gas-ions}$ on molality was sufficient to have good results.

$$k_{CO_2-Na^+} = -0.563937723 \cdot m_s - 4.352740149 \quad (13)$$

$$k_{CO_2-Cl^-} = 0.347571193 \cdot m_s + 4.762185508 \quad (14)$$

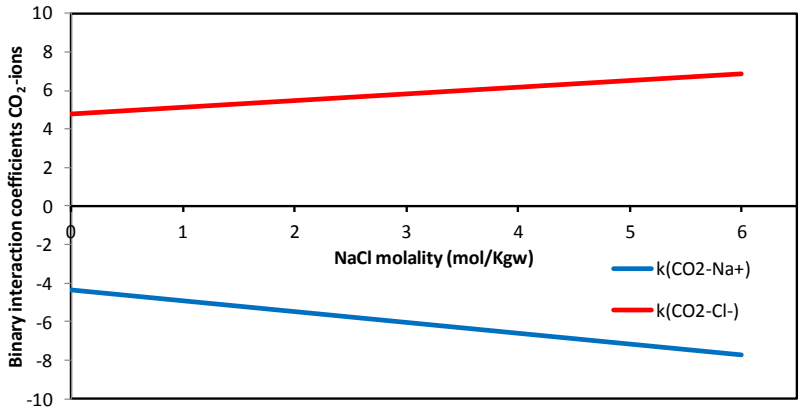


Figure 11 : Influence of molality on k_{CO_2-ions} for the H_2O-CO_2-NaCl system.

In Figure 12, the calculations done by e-PR-CPA, m-SW and geochemical models were compared with the experimental data (from literature and from this work) for the H_2O-CO_2-NaCl system. The experimental data measured in this work are in good agreement with the literature data (Figure 12-a) and also with model predictions (Figure 12-b). It should be noted that none of the measured data was included in the model parameterizations. The three models are in good agreement with the experimental data, and are able to estimate solubilities at high pressures and temperatures and for molalities up to saturation (~6m).

To compare the predictions of the three models over a wide range of temperature, pressure and molality, existing data in the open literature were collected [4, 7-12, 74-108]. The calculation was made for all the collected points (1150) and also at reduced temperature and pressure conditions in order to evaluate the predictions under the geological conditions of the storage. Calculations by the well-known DUAN model (Duan et al. [15]) were also done and compared with the other models. The Absolute Average Deviations (AAD) from the literature data in the different temperature and pressure ranges obtained with the models are summarized in Table 7. For all data, the geochemical model and the Duan model estimate solubility better than the m-SW and e-PR-CPA models, however, under storage conditions the e-PR-CPA model and the Duan model estimate solubility with an AAD less than 6.6%, while the m-SW model and the geochemical model estimate solubility with an AAD less than 7.6%. These results can be explained by the fact that the e-PR-CPA model and the m-SW model were adjusted only on data at temperatures between 313 and 433 K and therefore no liquid-liquid equilibrium data were included in the adjustment of these two models.

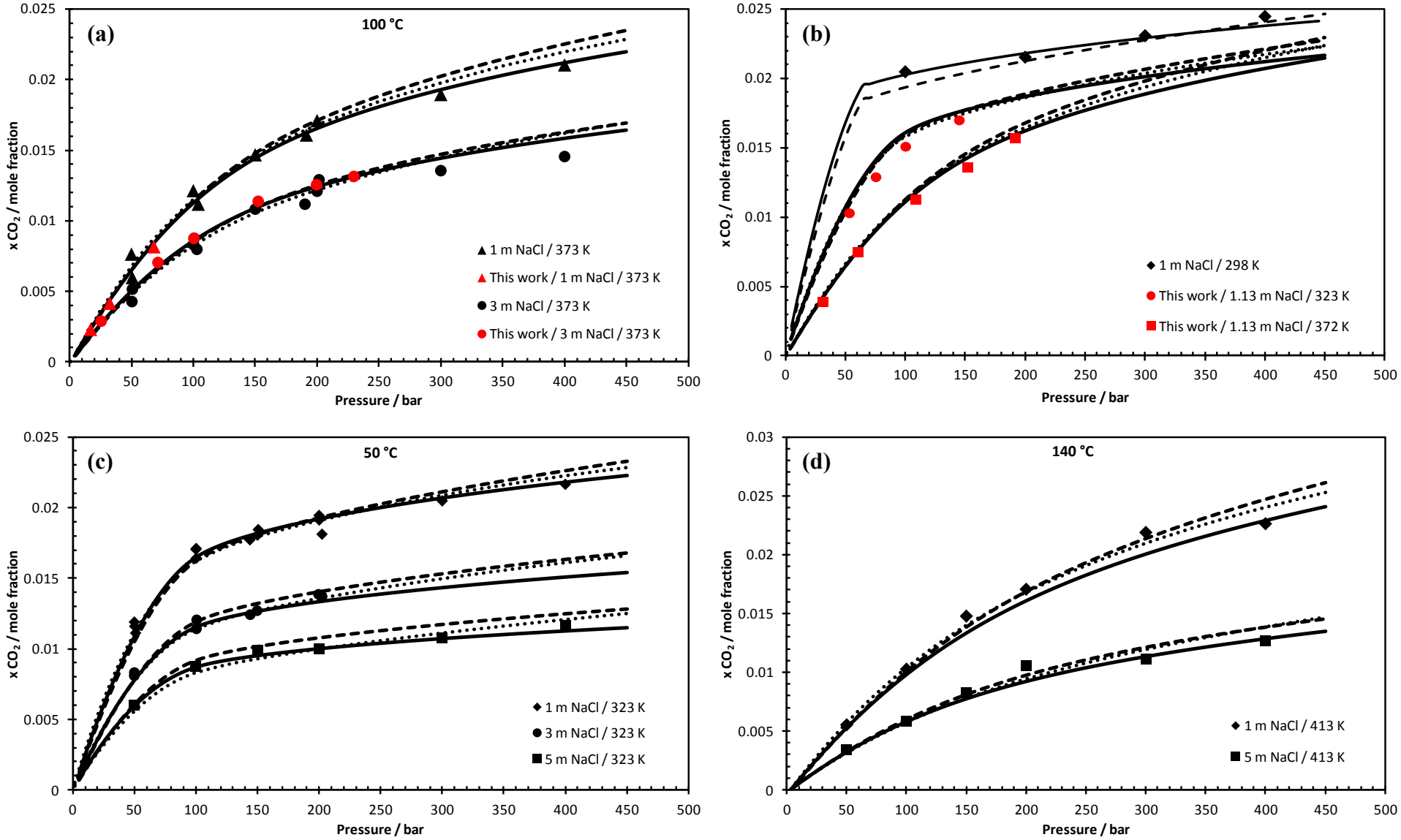


Figure 12 : CO_2-H_2O-NaCl system: Calculation of CO_2 solubility by e-PR-CPA (solid line), m-SW (dashed line) and geochemical (dotted line) models. The black symbols (a, b, c and d) are the literature data [4, 7, 11, 12], and the red symbols (a and b) are the measured data (Table 2).

Table 7 : Solubility of CO_2 in the CO_2-H_2O-NaCl system. AAD between experimental literature data and model predictions at different temperature and pressure ranges.

Selected data	Temperature (K)	Pressure (bars)	NaCl molality (mol/kgw)	Number of experimental points	AAD (%)			
					e-PR-CPA	m-SW	CHESS (Geoch.)	DUAN
All data	273.15 - 523.15	0.1 - 600	0 - 7.14	1150	10.2	10.2	6.7	6.4
Data at reduced temperature	297.00 - 433.08	1.9 - 600	0 - 7.14	725	7.0	7.3	7.5	6.6
Storage conditions	297.00 - 433.08	50 - 600	0 - 6.00	506	6.6	7.5	7.6	6.5

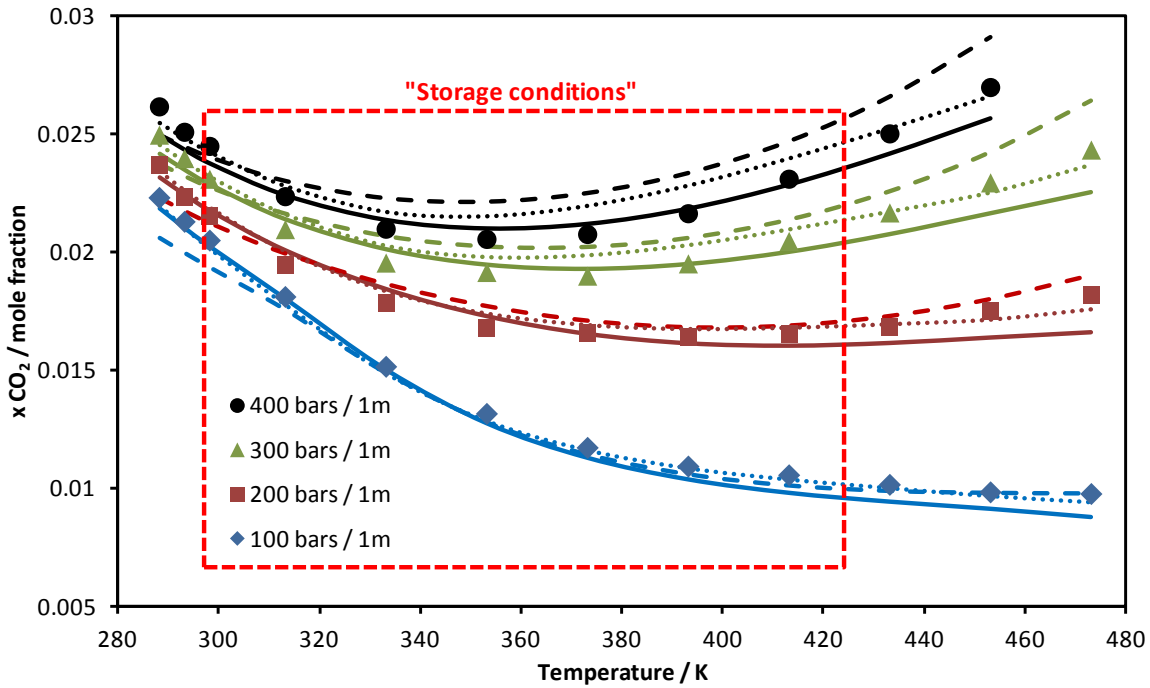


Figure 13 : CO_2-H_2O-NaCl system: Calculation of CO_2 solubility at different temperatures and pressures by e-PR-CPA (solid line), m-SW (dashed line) and geochemical (dotted line) models. The symbols are the literature data from Guo et al. [11].

The purpose of this comparison is to facilitate the choice of the appropriate model for an engineering application. The Duan model is widely used for the CO_2-brine system, but it is limited to a molality of 4.3 m (mol/kgw), therefore for storage applications in salt caverns (saturated brine), it is necessary to take the risk of extrapolation beyond the 4.3 m, which is not recommended with this type of empirical model. In this case, it is preferable to use the e-PR-CPA model (very accurate at high temperature and pressure, see Figures 12 and 13) or the geochemical model or Soreide and Whitson with the parameters proposed in this work (m-SW). To evaluate the models according to thermodynamic conditions (T and P), in Figure 13, calculations over a wide temperature and pressure range (at 1 m NaCl, more or less the salinity condition of aquifers) are presented and compared with literature data that have not been included in the model parameterization. At low temperature (below T_{c,CO_2}), where CO_2 is liquid (at high pressure), it is preferable to use the gamma-phi approach using the geochemical model, since in this approach each phase is represented by a specific model (SIT for the liquid phase, PR for the vapor phase). For reservoir simulation, it is necessary to carry out the stability test before the equilibrium calculation in each cell, this can only be done with an equation of state (phi-phi approach), it is known that for reservoir simulation, the number of points to be calculated is enormous (it can exceed one million points), which is why SAFT and CPA models are not used for this type of application given the high calculation time when comparing with cubic EoS. The m-SW model is best suited for reservoir simulation, and it is suggested to implement it according to the approach proposed by Petitfrere et al. [18] to solve the inconsistency problem and therefore use second order methods for the calculation of phase equilibria (Michelsen [109]). Finally, the common advantage of the models studied in this work is that they can generate reliable data without the need for more experimental measurements, which are generally complicated due to the presence of salts (corrosion, clogging, etc.) and require a lot of time and investment.

Conclusions

In this work, measurements of the solubility of carbon dioxide in NaCl brine were carried out by a new set-up based on the “static-analytic” method. A modification of the sampling procedure to avoid salt deposition in the sampler was made. The validation of this set-up was done by comparing some obtained results with the literature data. All measurements are intended to complement the existing data for this system, to evaluate and validate the developed models, and also to check the feasibility of sampling in saline solution. Our goal is to do measurement of solubility of mixture of gas.

The modeling of phase equilibria was carried out by four models using different approaches.

1- An improvement of the Soreide and Whitson model (m-SW) was made by proposing new correlations for binary interaction parameters. This model is implemented in many simulation software, so the old parameters can easily be replaced by those proposed in this work.

2- An electrolyte version of the PR-CPA model has been developed (e-PR-CPA) and parameterized on vapor pressure and osmotic coefficient data, to represent both equilibrium data and excess properties. For gas-water and gas-brine mixtures, the binary interaction parameters were adjusted on CO_2 solubility data.

3- A geochemical model implemented in CHESS/HYTEC software using an asymmetric "gamma-phi" approach was tested.

The liquid-vapor equilibria of the CO_2-H_2O system at very high pressure and temperature (up to the critical points of the mixture) were calculated by the e-PR-CPA model. CO_2 solubility and water content are well predicted, which proves the extrapolation quality with this model far from the adjustment range. The measurements performed in this work are in good agreement with the literature data and also with the model predictions. The e-PR-CPA, m-SW, geochemical and DUAN models reproduce the measured data with AAD of 4%, 4.5%, 6.6% and 6.9% respectively. A comparison of these models with all the existing literature data covering the geological storage conditions was carried out. In the storage condition the e-PR-CPA model and the Duan model reproduce solubilities with an AAD less than 6.6%, while the geochemical model and the m-SW model reproduce solubilities with an AAD less than 7.6%.

Finally, model predictions over a wide temperature and pressure range were compared with literature data to allow the evaluation of each model in a specific region (low and high pressure and temperature).

Nomenclature

a	energy parameter (Pa m^6 mol^{-2})
A	Helmholtz free energy, or Debye-Hückel parameter
$A_i,\ B_i$	site A or B in molecule i
b	molar co-volume (m^3/mol)
D	dielectric constant
D_0	vacuum permittivity (F/m)
e	elementary charge (C)
ea	electron acceptor site
ed	electron donor site
g	radial distribution function
I	ionic strength (mol/kgw)
k	binary interaction parameter
K	Henry's law constant
m	molality (mol/kgw), or e-PR-CPA parameter
M	Molar mass (kg/mol)
n	number of mole
N_{Av}	Avogadro number
P	pressure (Pa)
R	ideal gas constant (J mol^{-1} K^{-1})
T	temperature (K)
v	molar volume (m^3/mol)
V	volume (m^3)
x	liquid molar fraction
X	site fraction
y	vapor molar fraction
Z	electric charge

Greek letters

ε	CPA association energy (Pa m^3 mol^{-1}), or SIT binary interaction parameter
β	bonding volume
Δ	association strength
ρ	molar density (mol/m^3)
σ	ion diameter
γ	activity coefficient
φ	fugacity coefficient
ω	acentric factor
Γ	screening length

Subscripts

c	critical
g	gas
i, j	compound
liq	liquid
r	reduced
s	salt
sat	saturation
w	water

Superscripts

AQ	aqueous phase
cal	calculated value
exp	experimental value
g	gas
NA	non-aqueous phase
sf	salt-free
∞	infinite dilution

Abbreviations

BIP	Binary Interaction Parameter
CPA	Cubic Plus Association
DH	Debye-Hückel
EoS	Equation of State
MSA	Mean Spherical Approximation
NIST	National Institute of Standards and Technology
PR	Peng-Robinson
SIT	Specific Ion Theory
SW	Soreide and Whitson

Acknowledgments

Financial support from Agence Nationale de la Recherche (ANR) through the project FluidSTORY (n° 7747, ID ANR-15-CE06-0015) is gratefully acknowledged.

References

[1] P. Berest, Stockage souterrain des gaz et hydrocarbures : des perspectives pour la transition énergétique, Encyclopédie de l'Environnement [en ligne ISSN 2555-0950], (2019).
[2] O. Kruck, F. Crotogino, R. Prelicz, T. Rudolph, Assessment of the potential, the actors and relevant business cases for large scale and seasonal storage of renewable electricity by hydrogen underground storage in Europe, (2013).
[3] I. Søreide, C.H. Whitson, Peng-Robinson predictions for hydrocarbons, CO2, N2, and H2 S with pure water and NaCI brine, Fluid Phase Equilibria, 77 (1992) 217-240.
[4] D. Koschel, J.-Y. Coxam, L. Rodier, V. Majer, Enthalpy and solubility data of CO 2 in water and NaCl (aq) at conditions of interest for geological sequestration, Fluid phase equilibria, 247 (2006) 107-120.
[5] K. Tödheide, E. Franck, Das Zweiphasengebiet und die kritische Kurve im System Kohlendioxid–Wasser bis zu Drucken von 3500 bar, Zeitschrift für Physikalische Chemie, 37 (1963) 387-401.
[6] S. Takenouchi, G.C. Kennedy, The binary system H 2 O-CO 2 at high temperatures and pressures, American Journal of Science, 262 (1964) 1055-1074.
[7] W. Yan, S. Huang, E.H. Stenby, Measurement and modeling of CO2 solubility in NaCl brine and CO2–saturated NaCl brine density, International Journal of Greenhouse Gas Control, 5 (2011) 1460-1477.
[8] S.-X. Hou, G.C. Maitland, J.M. Trusler, Phase equilibria of (CO2+ H2O+ NaCl) and (CO2+ H2O+ KCl): Measurements and modeling, The Journal of Supercritical Fluids, 78 (2013) 78-88.
[9] H. Zhao, M.V. Fedkin, R.M. Dilmore, S.N. Lvov, Carbon dioxide solubility in aqueous solutions of sodium chloride at geological conditions: Experimental results at 323.15, 373.15, and 423.15 K and 150bar and modeling up to 573.15 K and 2000bar, Geochimica et Cosmochimica Acta, 149 (2015) 165-189.
[10] K. Gilbert, P.C. Bennett, W. Wolfe, T. Zhang, K.D. Romanak, CO 2 solubility in aqueous solutions containing Na+, Ca 2+, Cl−, SO 4 2− and HCO 3-: The effects of electrostricted water and ion hydration thermodynamics, Applied Geochemistry, 67 (2016) 59-67.
[11] H. Guo, Y. Huang, Y. Chen, Q. Zhou, Quantitative Raman Spectroscopic Measurements of CO2 Solubility in NaCl Solution from (273.15 to 473.15) K at p=(10.0, 20.0, 30.0, and 40.0) MPa, Journal of Chemical & Engineering Data, 61 (2015) 466-474.
[12] H. Messabeb, F.o. Contamine, P. Cézac, J.P. Serin, E.C. Gaucher, Experimental Measurement of CO2 Solubility in Aqueous NaCl Solution at Temperature from 323.15 to 423.15 K and Pressure of up to 20 MPa, Journal of Chemical & Engineering Data, 61 (2016) 3573-3584.
[13] J. Corvisier, Modeling water-gas-rock interactions using CHESS/HYTEC, in: Goldschmidt Conference, Florence–Italy, 2013.
[14] J. Corvisier, A.-F. Bonvalot, V. Lagneau, P. Chiquet, S. Renard, J. Sterpenich, J. Pironon, Impact of co-injected gases on CO2 storage sites: Geochemical modeling of experimental results, Energy Procedia, 37 (2013) 3699-3710.
[15] Z. Duan, R. Sun, C. Zhu, I.-M. Chou, An improved model for the calculation of CO2 solubility in aqueous solutions containing Na+, K+, Ca2+, Mg2+, Cl−, and SO42−, Marine Chemistry, 98 (2006) 131-139.
[16] E. El Ahmar, B. Creton, A. Valtz, C. Coquelet, V. Lachet, D. Richon, P. Ungerer, Thermodynamic study of binary systems containing sulphur dioxide: Measurements and molecular modelling, Fluid Phase Equilibria, 304 (2011) 21-34.
[17] D.-Y. Peng, D.B. Robinson, A new two-constant equation of state, Ind. Eng. Chem. Fundam., 15 (1976) 59.
[18] M. Petitfrere, L. Patacchini, R. de Loubens, Three-phase EoS-based Reservoir Simulation with Salinity Dependent Phase-equilibrium Calculations, in: ECMOR XV-15th European Conference on the Mathematics of Oil Recovery, 2016.
[19] G.M. Kontogeorgis, E.C. Voutsas, I.V. Yakoumis, D.P. Tassios, An equation of state for associating fluids, Industrial & engineering chemistry research, 35 (1996) 4310-4318.

[20] G. Soave, Equilibrium constants from a modified Redlich-Kwong equation of state, Chemical engineering science, 27 (1972) 1197-1203.
[21] M. Wertheim, Fluids with highly directional attractive forces. I. Statistical thermodynamics, Journal of statistical physics, 35 (1984) 19-34.
[22] D.B. Robinson, D.-Y. Peng, The characterization of the heptanes and heavier fractions for the GPA Peng-Robinson programs, Gas Processors Association, 1978.
[23] M. Hajiw, A. Chapoy, C. Coquelet, Hydrocarbons - water phase equilibria using the CPA equation of state with a group contribution method, The Canadian Journal of Chemical Engineering, 93 (2015) 432-442.
[24] T. Wang, E. El Ahmar, C. Coquelet, G.M. Kontogeorgis, Improvement of the PR-CPA equation of state for modelling of acid gases solubilities in aqueous alkanolamine solutions, Fluid Phase Equilibria, 471 (2018) 74-87.
[25] T. Wang, P. Guittard, C. Coquelet, E. El Ahmar, O. Baudouin, G. Kontogeorgis, Corrigendum to" Improvement of the PR-CPA equation of state for modelling of acid gases solubilities in aqueous alkanolamine solutions"[Fluid Phase Equilibria, Vol. 471, 2018, 74-87], Fluid Phase Equilibria, 485 (2019) 126-127.
[26] C. Held, T. Reschke, S. Mohammad, A. Luza, G. Sadowski, ePC-SAFT revised, Chemical Engineering Research and Design, 92 (2014) 2884-2897.
[27] B. Maribo-Mogensen, K. Thomsen, G.M. Kontogeorgis, An electrolyte CPA equation of state for mixed solvent electrolytes, AIChE Journal, 61 (2015) 2933-2950.
[28] D.K. Eriksen, G. Lazarou, A. Galindo, G. Jackson, C.S. Adjiman, A.J. Haslam, Development of intermolecular potential models for electrolyte solutions using an electrolyte SAFT-VR Mie equation of state, Molecular Physics, 114 (2016) 2724-2749.
[29] S. Ahmed, N. Ferrando, J.-C. De Hemptinne, J.-P. Simonin, O. Bernard, O. Baudouin, Modeling of mixed-solvent electrolyte systems, Fluid Phase Equilibria, 459 (2018) 138-157.
[30] R. Inchekel, J.-C. de Hemptinne, W. Fürst, The simultaneous representation of dielectric constant, volume and activity coefficients using an electrolyte equation of state, Fluid Phase Equilibria, 271 (2008) 19-27.
[31] B. Maribo-Mogensen, G.M. Kontogeorgis, K. Thomsen, Comparison of the Debye–Hückel and the Mean Spherical Approximation Theories for Electrolyte Solutions, Industrial & Engineering Chemistry Research, 51 (2012) 5353-5363.
[32] L. Blum, Mean spherical model for asymmetric electrolytes: I. Method of solution, Molecular Physics, 30 (1975) 1529-1535.
[33] M. Born, Volumen und hydratationswärme der ionen, Zeitschrift für Physik, 1 (1920) 45-48.
[34] A. Anderko, K.S. Pitzer, Equation-of-state representation of phase equilibria and volumetric properties of the system NaCl-H2O above 573 K, Geochimica et Cosmochimica Acta, 57 (1993) 1657-1680.
[35] D. Tong, J.M. Trusler, D. Vega-Maza, Solubility of CO2 in aqueous solutions of CaCl2 or MgCl2 and in a synthetic formation brine at temperatures up to 423 K and pressures up to 40 MPa, Journal of Chemical & Engineering Data, 58 (2013) 2116-2124.
[36] W.H. Press, FORTRAN Numerical Recipes: Numerical recipes in FORTRAN 90: the art of parallel scientific computing, Cambridge University Press, 1996.
[37] S.H. Huang, M. Radosz, Equation of state for small, large, polydisperse, and associating molecules, Industrial & Engineering Chemistry Research, 29 (1990) 2284-2294.
[38] W. Wagner, A. Pruß, The IAPWS formulation 1995 for the thermodynamic properties of ordinary water substance for general and scientific use, Journal of physical and chemical reference data, 31 (2002) 387-535.
[39] N. Hubert, Y. Gabes, J.-B. Bourdet, L. Schuffenecker, Vapor pressure measurements with a nonisothermal static method between 293.15 and 363.15 K for electrolyte solutions. Application to the H2O+ NaCl system, Journal of Chemical and Engineering Data, 40 (1995) 891-894.
[40] J.L. Haas Jr, Thermodynamics properties of the coexisting phases and thermochemical properties of the NaCl component in boiling NaCl solutions, US, Geol. Surv., Bull.;(United States), 1421 (1976).

[41] W.J. Hamer, Y.C. Wu, Osmotic coefficients and mean activity coefficients of uni-univalent electrolytes in water at 25° C, Journal of Physical and Chemical Reference Data, 1 (1972) 1047-1100.
[42] J.A. Rard, D.G. Archer, Isopiestic Investigation of the Osmotic and Activity Coefficients of Aqueous NaBr and the Solubility of NaBr. cntdot. 2H2O (cr) at 298.15 K: Thermodynamic Properties of the NaBr+ H2O System over Wide Ranges of Temperature and Pressure, Journal of Chemical and Engineering Data, 40 (1995) 170-185.
[43] J. llmari Partanen, P.O. Minkkinen, Thermodynamic Activity Quantities in Aqueous Sodium and Potassium Chloride Solutions at 298.15 K up to a Molality of 2.0 mol kg _1, Acta Chemica Scandinavica, 47 (1993) 768-776.
[44] R.A. Robinson, R.H. Stokes, Tables of osmotic and activity coefficients of electrolytes in aqueous solution at 25 C, Transactions of the Faraday Society, 45 (1949) 612-624.
[45] H.F. Gibbard Jr, G. Scatchard, R.A. Rousseau, J.L. Creek, Liquid-vapor equilibrium of aqueous sodium chloride, from 298 to 373. deg. K and from 1 to 6 mol kg-1, and related properties, Journal of Chemical and Engineering Data, 19 (1974) 281-288.
[46] K.S. Pitzer, J.C. Peiper, R. Busey, Thermodynamic properties of aqueous sodium chloride solutions, Journal of Physical and Chemical Reference Data, 13 (1984) 1-102.
[47] K.S. Pitzer, Thermodynamics of electrolytes. I. Theoretical basis and general equations, The Journal of Physical Chemistry, 77 (1973) 268-277.
[48] K.S. Pitzer, Ion interaction approach: theory and data correlation, Activity coefficients in electrolyte solutions, 2 (1991) 75-153.
[49] J.N. Brønsted, Studies on solubility. IV. The principle of the specific interaction of ions, Journal of the American Chemical Society, 44 (1922) 877-898.
[50] G. Scatchard, Concentrated Solutions of Strong Electrolytes, Chemical Reviews, 19 (1936) 309-327.
[51] E. Guggenheim, J. Turgeon, Specific interaction of ions, Transactions of the Faraday Society, 51 (1955) 747-761.
[52] P. Debye, E. Hückel, De la theorie des electrolytes. I. abaissement du point de congelation et phenomenes associes, Physikalische Zeitschrift, 24 (1923) 185-206.
[53] I. Grenthe, I. Puigdomenech, B. Allard, Modelling in aquatic chemistry, OECD Publishing, 1997.
[54] M. Hajiw, J. Corvisier, E. El Ahmar, C. Coquelet, Impact of impurities on CO 2 storage in saline aquifers: Modelling of gases solubility in water, International Journal of Greenhouse Gas Control, 68 (2018) 247-255.
[55] A.C. Schneider, C. Pasel, M. Luckas, K.G. Schmidt, J.-D. Herbell, Determination of hydrogen single ion activity coefficients in aqueous HCl solutions at 25 C, Journal of solution chemistry, 33 (2004) 257-273.
[56] H. Sakaida, T. Kakiuchi, Determination of single-ion activities of H+ and Cl–in aqueous hydrochloric acid solutions by use of an ionic liquid salt bridge, The Journal of Physical Chemistry B, 115 (2011) 13222-13226.
[57] M.K. Khoshkbarchi, J.H. Vera, Measurement and correlation of ion activity in aqueous single electrolyte solutions, AIChE journal, 42 (1996) 249-258.
[58] R. Wiebe, V. Gaddy, The solubility in water of carbon dioxide at 50, 75 and 100, at pressures to 700 atmospheres, Journal of the American Chemical Society, 61 (1939) 315-318.
[59] S.-X. Hou, G.C. Maitland, J.M. Trusler, Measurement and modeling of the phase behavior of the (carbon dioxide+ water) mixture at temperatures from 298.15 K to 448.15 K, The Journal of Supercritical Fluids, 73 (2013) 87-96.
[60] A. Bamberger, G. Sieder, G. Maurer, High-pressure (vapor+ liquid) equilibrium in binary mixtures of (carbon dioxide+ water or acetic acid) at temperatures from 313 to 353 K, The Journal of Supercritical Fluids, 17 (2000) 97-110.
[61] R. Dohrn, A. Bünz, F. Devlieghere, D. Thelen, Experimental measurements of phase equilibria for ternary and quaternary systems of glucose, water, CO2 and ethanol with a novel apparatus, Fluid Phase Equilibria, 83 (1993) 149-158.

[62] P. Ahmadi, A. Chapoy, CO2 solubility in formation water under sequestration conditions, Fluid Phase Equilibria, 463 (2018) 80-90.
[63] J. Briones, J. Mullins, M. Thies, B.-U. Kim, Ternary phase equilibria for acetic acid-water mixtures with supercritical carbon dioxide, Fluid Phase Equilibria, 36 (1987) 235-246.
[64] A.D. King Jr, C. Coan, Solubility of water in compressed carbon dioxide, nitrous oxide, and ethane. Evidence for hydration of carbon dioxide and nitrous oxide in the gas phase, Journal of the American Chemical Society, 93 (1971) 1857-1862.
[65] K. Jackson, L.E. Bowman, J.L. Fulton, Water solubility measurements in supercritical fluids and high-pressure liquids using near-infrared spectroscopy, Analytical Chemistry, 67 (1995) 2368-2372.
[66] G. Müller, E. Bender, G. Maurer, Das Dampf-Flüssigkeitsgleichgewicht des ternären Systems Ammoniak-Kohlendioxid-Wasser bei hohen Wassergehalten im Bereich zwischen 373 und 473 Kelvin, Berichte der Bunsengesellschaft für physikalische Chemie, 92 (1988) 148-160.
[67] A. Valtz, A. Chapoy, C. Coquelet, P. Paricaud, D. Richon, Vapour–liquid equilibria in the carbon dioxide–water system, measurement and modelling from 278.2 to 318.2 K, Fluid phase equilibria, 226 (2004) 333-344.
[68] M. King, A. Mubarak, J. Kim, T. Bott, The mutual solubilities of water with supercritical and liquid carbon dioxides, The Journal of Supercritical Fluids, 5 (1992) 296-302.
[69] T. Nakayama, H. Sagara, K. Arai, S. Saito, High pressure liquid・ liquid equilibria for the system of water, ethanol and 1, 1-difluoroethane at 323.2 K, Fluid Phase Equilibria, 38 (1987) 109-127.
[70] P. Gillespie, G. Wilson, GPA Research Report RR-48, Gas Processors Association, Tulsa, (1982).
[71] H. Greenwood, H. Barnes, SECTION 17: BINARY MIXTURES OF VOLATILE COMPONENTS, Geological Society of America Memoirs, 97 (1966) 385-400.
[72] R. Wiebe, V. Gaddy, Vapor phase composition of carbon dioxide-water mixtures at various temperatures and at pressures to 700 atmospheres, Journal of the American Chemical Society, 63 (1941) 475-477.
[73] P. Van Konynenburg, R. Scott, Critical lines and phase equilibria in binary van der Waals mixtures, Philosophical Transactions of the Royal Society of London. Series A, Mathematical and Physical Sciences, 298 (1980) 495-540.
[74] B. Rumpf, H. Nicolaisen, C. Öcal, G. Maurer, Solubility of carbon dioxide in aqueous solutions of sodium chloride: experimental results and correlation, Journal of solution chemistry, 23 (1994) 431-448.
[75] J.J. Mackenzie, Ueber die Absorption der Gase durch Salzlösungen, Annalen der Physik, 237 (1877) 438-451.
[76] M. Setschenow, Action de l'acide carbonique sur les solutions dessels a acides forts. Etude absortiometrique, Ann. Chim. Phys, 25 (1892) 226-270.
[77] K.A. Kobe, J.S. Williams, Confining liquids for gas analysis: solubility of carbon dioxide in salt solutions, Industrial & Engineering Chemistry Analytical Edition, 7 (1935) 37-38.
[78] A.E. Markham, K.A. Kobe, The solubility of carbon dioxide and nitrous oxide in aqueous salt solutions, Journal of the American Chemical Society, 63 (1941) 449-454.
[79] H.S. Harned, R. Davis Jr, The ionization constant of carbonic acid in water and the solubility of carbon dioxide in water and aqueous salt solutions from 0 to 50, Journal of the American Chemical Society, 65 (1943) 2030-2037.
[80] W. Rosenthal, thesis, in: Faculty of Science, University of Strasbourg, 1954.
[81] A. Ellis, R. Golding, The solubility of carbon dioxide above 100 degrees C in water and in sodium chloride solutions, American Journal of Science, 261 (1963) 47-60.
[82] S.Y. Yeh, R.E. Peterson, Solubility of carbon dioxide, krypton, and xenon in aqueous solution, Journal of pharmaceutical sciences, 53 (1964) 822-824.
[83] S. Takenouchi, G.C. Kennedy, The solubility of carbon dioxide in NaCl solutions at high temperatures and pressures, American journal of science, 263 (1965) 445-454.
[84] K. ONDA, E. SADA, T. KOBAYASHI, S. KITO, K. ITO, Salting-out parameters of gas solubility in aqueous salt solutions, Journal of Chemical Engineering of Japan, 3 (1970) 18-24.

[85] Y.H. Li, T.F. Tsui, The solubility of CO2 in water and sea water, Journal of Geophysical research, 76 (1971) 4203-4207.
[86] S. Malinin, N. Savelyeva, Experimental investigations of CO2 solubility in NaCl and CaCl2 solutions at temperature of 25, 50 and 75 Degrees and elevated CO2 pressure, Geochem. Int, 9 (1972) 643.
[87] S. Malinin, N. Kurovskaya, Solubility of CO2 in chloride solutions at elevated temperatures and CO2 pressures, Geochem. Int, 12 (1975) 199-201.
[88] A. Yasunishi, F. Yoshida, Solubility of carbon dioxide in aqueous electrolyte solutions, Journal of Chemical and Engineering Data, 24 (1979) 11-14.
[89] S. Drummond, Boiling and mixing of hydrothermal fluids: Effects on mineral deposition, in, Ph. D. thesis, Pennsylvania State University, 1981.
[90] G. Burmakina, L. Efanov, M. Shnet, CO2 SOLUBILITY IN AQUEOUS-SOLUTIONS OF SOME ELECTROLYTES AND SUCROSE, ZHURNAL FIZICHESKOI KHIMII, 56 (1982) 1159-1161.
[91] S. Cramer, Solubility of methane, carbon dioxide, and oxygen in brines from 0/sup 0/to 300/sup 0/C, in, Bureau of Mines, Pittsburgh, PA, 1982.
[92] M. Gehrig, H. Lentz, E. Franck, The system water—carbon dioxide—sodium chloride to 773 K and 300 MPa, Berichte der Bunsengesellschaft für physikalische Chemie, 90 (1986) 525-533.
[93] J.A. Nighswander, N. Kalogerakis, A.K. Mehrotra, Solubilities of carbon dioxide in water and 1 wt.% sodium chloride solution at pressures up to 10 MPa and temperatures from 80 to 200. degree. C, Journal of Chemical and Engineering Data, 34 (1989) 355-360.
[94] S. He, J.W. Morse, The carbonic acid system and calcite solubility in aqueous Na-K-Ca-Mg-Cl-SO4 solutions from 0 to 90°C, Geochimica et Cosmochimica Acta, 57 (1993) 3533-3554.
[95] G. Vazquez, F. Chenlo, G. Pereira, CO2 DIFFUSIVITY IN NACL AND CUSO4 AQUEOUS-SOLUTIONS, Afinidad, 51 (1994) 369-374.
[96] G. Vázquez, F. Chenlo, G. Pereira, J. Peaguda, SOLUBILITY OF CO2 IN AQUEOUS-SOLUTIONS OF NACL, CUSO4, KL AND NABR, in: Anales de Quimica, REAL SOC ESPAN QUIMICA FACULTAD DE FISICA QUIMICA CIUDAD UNIV, 3 MADRID, SPAIN, 1994, pp. 324-328.
[97] D.-Q. Zheng, T.-M. Guo, H. Knapp, Experimental and modeling studies on the solubility of CO2, CHC1F2, CHF3, C2H2F4 and C2H4F2 in water and aqueous NaCl solutions under low pressures, Fluid Phase Equilibria, 129 (1997) 197-209.
[98] J. Kiepe, S. Horstmann, K. Fischer, J. Gmehling, Experimental determination and prediction of gas solubility data for CO2+ H2O mixtures containing NaCl or KCl at temperatures between 313 and 393 K and pressures up to 10 MPa, Industrial & Engineering Chemistry Research, 41 (2002) 4393-4398.
[99] S. Bando, F. Takemura, M. Nishio, E. Hihara, M. Akai, Solubility of CO2 in aqueous solutions of NaCl at (30 to 60) C and (10 to 20) MPa, Journal of Chemical & Engineering Data, 48 (2003) 576-579.
[100] G. Ferrentino, D. Barletta, F. Donsì, G. Ferrari, M. Poletto, Experimental measurements and thermodynamic modeling of CO2 solubility at high pressure in model apple juices, Industrial & Engineering Chemistry Research, 49 (2010) 2992-3000.
[101] Y. Liu, M. Hou, G. Yang, B. Han, Solubility of CO2 in aqueous solutions of NaCl, KCl, CaCl2 and their mixed salts at different temperatures and pressures, The Journal of supercritical fluids, 56 (2011) 125-129.
[102] J. Rosenqvist, A.D. Kilpatrick, B.W. Yardley, Solubility of carbon dioxide in aqueous fluids and mineral suspensions at 294 K and subcritical pressures, Applied geochemistry, 27 (2012) 1610-1614.
[103] V. Savary, G. Berger, M. Dubois, J.-C. Lacharpagne, A. Pages, S. Thibeau, M. Lescanne, The solubility of CO2+ H2S mixtures in water and 2 M NaCl at 120° C and pressures up to 35 MPa, International Journal of Greenhouse Gas Control, 10 (2012) 123-133.
[104] C. Langlais, Impacts géochimiques de la présence d'oxygène sur les saumures en conditions de stockage géologique de CO2 : caractérisation de solubilités, in, 2013.
[105] P.J. Carvalho, L.M. Pereira, N.P. Gonçalves, A.J. Queimada, J.A. Coutinho, Carbon dioxide solubility in aqueous solutions of NaCl: Measurements and modeling with electrolyte equations of state, Fluid Phase Equilibria, 388 (2015) 100-106.

[106] E. Mohammadian, H. Hamidi, M. Asadullah, A. Azdarpour, S. Motamedi, R. Junin, Measurement of CO2 solubility in NaCl brine solutions at different temperatures and pressures using the potentiometric titration method, Journal of Chemical & Engineering Data, 60 (2015) 2042-2049.
[107] R. Jacob, B.Z. Saylor, CO2 solubility in multi-component brines containing NaCl, KCl, CaCl2 and MgCl2 at 297 K and 1–14 MPa, Chemical Geology, 424 (2016) 86-95.
[108] B. Liborio, Dissolution du dioxyde de carbone dans des solutions aqueuses d'électrolyte dans le contexte du stockage géologique : approche thermodynamique, in, 2017.
[109] M.L. Michelsen, The isothermal flash problem. Part II. Phase-split calculation, Fluid phase equilibria, 9 (1982) 21-40.
[110] G. Soave, Equilibrium constants from a modified Redlich-Kwong equation of state, Chem. Eng. Sci., 27 (1972) 1197-1203.
[111] M. Michelsen, J. Mollerup, Thermodynamic models: fundamentals & computational aspects. 2004, Holte, Denmark: Tie-Line Publications.
[112] X. Courtial, N. Ferrando, J.-C. De Hemptinne, P. Mougin, Electrolyte CPA equation of state for very high temperature and pressure reservoir and basin applications, Geochimica et Cosmochimica Acta, 142 (2014) 1-14.
[113] W. Fürst, H. Renon, Representation of excess properties of electrolyte solutions using a new equation of state, AIChE Journal, 39 (1993) 335-343.
[114] G.M. Kontogeorgis, G.K. Folas, Thermodynamic models for industrial applications: from classical and advanced mixing rules to association theories, John Wiley & Sons, 2009.
[115] G.K. Folas, J. Gabrielsen, M.L. Michelsen, E.H. Stenby, G.M. Kontogeorgis, Application of the Cubic-Plus-Association (CPA) Equation of State to Cross-Associating Systems, Ind. Eng. Chem. Res., 44 (2005) 3823-3833.
[116] F.X. Ball, H. Planche, W. Fürst, H. Renon, Representation of deviation from ideality in concentrated aqueous solutions of electrolytes using a mean spherical approximation molecular model, AIChE journal, 31 (1985) 1233-1240.
[117] J.A. Myers, S.I. Sandler, R.H. Wood, An equation of state for electrolyte solutions covering wide ranges of temperature, pressure, and composition, Industrial & engineering chemistry research, 41 (2002) 3282-3297.
[118] J.-P. Simonin, O. Bernard, L. Blum, Real ionic solutions in the mean spherical approximation. 3. Osmotic and activity coefficients for associating electrolytes in the primitive model, The Journal of Physical Chemistry B, 102 (1998) 4411-4417.
[119] M. Uematsu, E. Frank, Static dielectric constant of water and steam, Journal of Physical and Chemical Reference Data, 9 (1980) 1291-1306.

Appendix A: Soreide and Whitson EoS

The PR EoS is expressed as

$$P(T,v) = \frac{RT}{v-b} - \frac{a(T)}{v(v+b)+b(v-b)} \tag{15}$$

where P is the pressure, T the temperature, R the ideal gas constant, v the molar volume. The energy parameter a and the molar co-volume b for a pure compound i are given by

$$a_i(T) = 0.457235529\frac{R^2T_{c,i}^2}{P_{c,i}} \times \alpha(T) \tag{16}$$

$$b_i = 0.0777960739\frac{RT_{c,i}}{P_{c,i}} \tag{17}$$

In Eqs. (16) and (17), $P_{c,i}$ and $T_{c,i}$ are respectively the critical pressure and the critical temperature of compound i.

The modifications applied by Soreide and Whitson (SW) are as follows:

- The first modification concerns the alpha function $\alpha(T)$:

The generalized alpha function proposed by Soave [110] has been selected for gases:

$$\alpha_g(T) = \left[1 + 0.37464 + 1.54226\omega_i - 0.26992{\omega_i}^2\left(1 - \sqrt{\frac{T}{T_{c,i}}}\right)\right]^2 \tag{18}$$

where ω_i is the acentric factor. For CO_2, the critical properties and acentric factor used in this work are:

$T_{c,CO_2} = 304.13$ K, $P_{c,CO_2} = 73.773$ bar and $\omega_{CO_2} = 0.22394$

To improve the vapor pressure of water + brine, a specific alpha function for α_w depending on the reduced temperature and NaCl molality m_s was proposed, and is given by:

$$\alpha_w(T) = \left[1 + 0.4530\left[1 - \frac{T}{T_{c,w}}(1 - 0.0103\ \mathrm{m_s^{1.1}})\right] + 0.0034\left(\left(\frac{T}{T_{c,w}}\right)^{-3} - 1\right)\right]^2 \tag{19}$$

The alpha function α in the Eq. (16) is equal to α_g for gases and to α_w for water or brine.

- The second modification concerns the mixing rules:

The classical mixing rules have been used with two different binary interaction parameters (k_{ij}). The first one is for the aqueous phase and the second one is for the gas phase (liquid-vapor equilibrium) or the other liquid phase (liquid-liquid equilibrium):

$$a_m^{AQ}(T) = \sum_{i=1}^{n_c}\sum_{i=1}^{n_c} x_i x_j \sqrt{a_i(T)a_j(T)}\left(1 - k_{ij}^{AQ}\right) \tag{20}$$

$$a_m^{NA}(T) = \sum_{i=1}^{n_c}\sum_{i=1}^{n_c} y_i y_j \sqrt{a_i(T)a_j(T)}(1 - k_{ij}^{NA}) \tag{21}$$

a_m^{NA} is the attractive parameter of the gas-rich phase (hydrocarbon, acid gas, H_2, etc.), $a_m^{AQ}$is the attractive parameter of the water-rich phase (aqueous phase).

Appendix B: e-PR-CPA EoS

The e-PR-CPA model (Eq. (7)) is composed of different contributions to the Helmholtz energy A. By deriving A with respect to T, V and n, all other thermodynamic properties can be calculated; the procedure is detailed in the book by Michelsen and Mollerup [111]. Below the different terms are presented.

$$\frac{A^{PR}}{RT} = -\ln\left(1 - \frac{b}{v}\right) - \frac{a(T)}{2\sqrt{2}RTb}\ln\left(\frac{1 + \left(1 + \sqrt{2}\right)\frac{b}{v}}{1 + \left(1 - \sqrt{2}\right)\frac{b}{v}}\right) \tag{22}$$

The energy parameter $a(T)$ for the pure (non-ionic) compound i is obtained by the following equation:

$$a_i = a_{0,i} \times \left[1 + m_i\left(1 - \sqrt{\frac{T}{T_{c,i}}}\right)\right]^2 \tag{23}$$

For non-associative pure compounds (gases in our case), a_i is obtained by Eqs. (16) and (18). For associative compounds such as water, these three parameters are adjusted to pure component experimental data.

Critical temperatures of ionic compounds are unknown. Courtial et al. [112] proposed to replace the critical temperature in Eq. (23) by the reference temperature 298.15 K for ions,

since the majority of the available data are at this temperature. For ionic species the Eq. (23) becomes

$$a_{ion} = a_{0,ion} \times \left[1 + m_{ion}\left(1 - \sqrt{\frac{T}{298.15}}\right)\right]^2 \tag{24}$$

The co-volume b of an ion is related to its diameter σ_{ion} (adjustable parameter) with the relationship proposed by Fürst and Renon [113]:

$$b_{ion} = \frac{N_{Av}\pi(\sigma_{ion})^3}{6} \tag{25}$$

where N_{Av} is the Avogadro number. The adjustable parameters for each ion are $a_{0,ion}$, m_{ion} and σ_{ion}.

For mixtures a and b are determined by the van der Waals classical mixing rules:

$$a = \sum_i \sum_j x_i x_j \sqrt{a_i a_j}\left(1 - k_{ij}\right) \tag{26}$$

$$b = \sum_i x_i b_i \tag{27}$$

where x_i is the molar fraction of species i and k_{ij} the binary interaction parameter between species i and j (i and j can be either ions or molecules).

$$\frac{A^{Association}}{RT} = \sum_i n_i \sum_{A^i}\left(\ln\left(X_{A_i}\right) + \frac{1 - X_{A_i}}{2}\right) \tag{28}$$

In Eq. (28), n_i stands for the number of mole of component i; X_{A_i} is the fraction of sites of type A in molecule i that are non bonded, and is obtained by solving the following equations:

$$X_{A_i} = \frac{1}{1 + \rho \sum_j x_j \sum_{B_j} X_{B_j} \Delta^{A_i B_j}} \tag{29}$$

where $\rho = \frac{1}{v}$ stands for the molar density. $\Delta^{A_i B_j}$ is the association strength between sites A_i and B_j of molecules i and j, and is determined by the following equation.

$$\Delta^{A_iB_j} = g(\rho)\left[\exp\left(\frac{\varepsilon^{A_iB_j}}{RT}\right)\right] b_{ij}\,\beta^{A_iB_j} \tag{30}$$

where:

$$b_{ij} = \frac{b_i + b_j}{2} \tag{31}$$

g is the radial distribution function [19] at contact, which is given by:

$$g(\rho) = \frac{1}{1-1.9\,\eta} \tag{32}$$

with $\eta = \frac{1}{4} b\rho$

The association energy $\varepsilon^{A_iB_j}$ and the bonding volume $\beta^{A_iB_j}$ are two adjustable parameters for pure self-associating compounds. For mixtures, some combining rules are used to the cross association parameters. Generally, the CR1 [114] combining rules are used in the case of a mixture with two self-associating fluids:

$$\varepsilon^{A_iB_j} = \frac{\varepsilon^{A_iB_i} + \varepsilon^{A_jB_j}}{2} \tag{33}$$

$$\beta^{A_iB_j} = \sqrt{\beta^{A_iB_i}\beta^{A_jB_j}} \tag{34}$$

In the case of solvation of a non self-associating fluid by a self-associating fluid (water, alcohol, etc.), the modified combining rules (m-CR1) proposed by Folas et al. [115] can be used:

$$\varepsilon^{A_iB_j} = \frac{\varepsilon_{associating}}{2} \tag{35}$$

while the parameter

$\beta^{A_iB_j}$ is adjusted to mixture experimental data. (36)

Long-range electrostatic forces (Coulomb interaction) are described by the MSA term $\left(\frac{A^{MSA}}{RT}\right)$. In this work we use the form proposed by Ball et al. [116] (Eq. (37)), which is a simplified version of the non restricted primitive MSA (nRP-MSA) developed by Blum [32]. The nRP-MSA model treats ions as charged hard spheres of different diameters and considers the solvent as a dielectric continuum through its dielectric constant D.

$$\frac{A^{MSA}}{RT} = -\frac{\alpha_{MSA}^2}{4\pi}\sum_i \frac{n_i Z_i^2 \Gamma}{1+\Gamma\sigma_i} + \frac{V\Gamma^3}{3\pi N_{Av}} \tag{37}$$

where:

$$\alpha_{MSA}^2 = \frac{N_{Av}e^2}{D_0 DRT} \tag{38}$$

where e is the elementary charge, n_i is the number of moles of the ion i, D_0 is the vacuum permittivity and Z_i is the electric charge of species i.

The screening length Γ is determined from the iterative resolution of the following equation.

$$4\Gamma^2 = \alpha_{MSA}^2 N_{Av}\sum_i \frac{n_i}{V}\left(\frac{Z_i}{1+\Gamma\sigma_i}\right)^2 \tag{39}$$

The Born's term $\frac{A^{Born}}{RT}$ (Eq. (40)) [117] describes the short-range interactions (ion solvation). This contribution quantifies the energy of solvation by calculating the energy required to transfer an ion from the vacuum to a solvent of dielectric constant D [114]. It is given by

$$\frac{A^{Born}}{RT} = -\frac{N_{Av}e^2}{4\pi D_0 RT}\left(1-\frac{1}{D}\right)\sum_i \frac{n_i Z_i^2}{\sigma_i} \tag{40}$$

In both electrolyte terms (Born and MSA), the dielectric constant D must be determined. Inchekel et al. [30] showed that the Born term has an effect of the activity coefficients of the species as long as the dielectric constant depends on the concentration of salts. In this word, we use Simonin's model [118] to compute the dielectric constant D of the electrolyte solution:

$$D = \frac{D_s}{1+\alpha\sum_i^{ions} x_i} \tag{41}$$

where α is salt dependent adjustable parameter. The value of 5.08 proposed by Inchekel et al. [30] for the H_2O+NaCl system is used in this work. D_s is the dielectric constant of the pure solvent (water in our case). The correlation proposed by Uematsu and Franck [119] was used to determine D_s:

$$\begin{aligned} D_s = 1 &+ \left(\frac{7.62571}{T^*}\right)\rho^* + \left(\frac{244.003}{T^*} - 140.569 + 27.7841T^*\right)\rho^{*2} \\ &+ \left(\frac{-96.2805}{T^*} + 41.7909T^* - 10.2099T^{*2}\right)\rho^{*3} \\ &+ \left(\frac{-45.2059}{T^{*2}} + \frac{84.6395}{T^*} - 35.8644\right)\rho^{*4} \end{aligned} \tag{42}$$

where $T^* = \frac{T}{T_0}$ and $\rho^* = \frac{\rho_w}{\rho_0}$ with $T_0 = 298.15\ K$ and $\rho_0 = 1000\ kg/m^3$. T is the temperature (in K), ρ_w is the density of pure water (in kg/m^3).

As suggested by Myers et al. [117], the water density used in Eq. (42) is calculated from the number of moles of water in the solution n_w and the volume of the solution V, as

$$\rho_w = \frac{n_w M_{H_2O}}{V} \tag{43}$$

where $\mathrm{M_{H_2O}}$ is the molar mass of water in kg/mol.